2-P

SPACE DIVISION

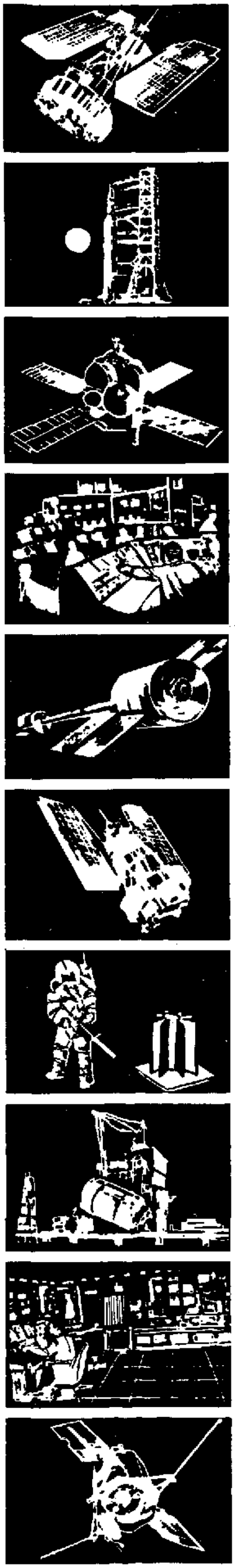

CR 134307

STUDY OF RECRYSTALLIZATION AND DEVITRIFICATION OF LUNAR GLASS

BY DONALD R. ULRICH

(NASA-CR-134307) STUDY OF RECRYSTALLIZATION AND DEVITRIFICATION OF LUNAR GLASS Final Report (General Electric Co.) 58 p HC $6.00 CSCL 11D
N74-27040
Unclas
G3/18 41296

CONTRACT NAS 8–12654

PREPARED FOR THE
NATIONAL AERONAUTICS AND SPACE ADMINISTRATION
JOHNSON SPACE CENTER
HOUSTON, TEXAS

GENERAL ELECTRIC

58

STUDY OF RECRYSTALLIZATION AND DEVITRIFICATION OF LUNAR GLASS

BY DONALD R. ULRICH

FINAL REPORT

APRIL 1974

CONTRACT NAS 8–12654

PREPARED FOR THE

NATIONAL AERONAUTICS AND SPACE ADMINISTRATION
JOHNSON SPACE CENTER
HOUSTON, TEXAS

PREPARED BY
SPACE SCIENCES LABORATORY

GENERAL ELECTRIC

SPACE DIVISION

Valley Forge Space Center

P. O. Box 8555 • Philadelphia, Penna. 19101

TABLE OF CONTENTS

LIST OF ILLUSTRATIONS

LIST OF TABLES

FOREWORD

This report was prepared for the NASA-Johnson Space Center by the Space Sciences Laboratory, General Electric Company, Philadelphia, Pennsylvania, under contract NAS 9-12654, "Study of Recrystallization and Devitrification of Lunar Glass." The research was carried out under the supervision of Dr. Donald R. Ulrich, Principal Investigator.

Contributions were made by several scientific collaborators over the course of the program. At the Space Sciences Laboratory they were Dr. Edward C. Henry, Dr. Barry A. Noval, Dr. Michael J. Noone, Dr. Earl Feingold, Mr. Harry W. Rauch, Sr., Mr. Ralph W. Gunnett, Mr. T. Harris and Mrs. Barbara Faust. Scanning electron microscopy contributions were made by Mr. William Leyshon, Dr. Walter Brouillett, and Mr. John Devore of the General Electric Electronics Laboratory, Syracuse, New York.

Co-investigator and geological consultant was Dr. Jon Weber, Professor of Geochemistry, Pennsylvania State University, University Park, Penna.

Acknowledgement is extended to Dr. John Harris, NASA-Johnson Space Center, and Dr. John Pomeroy, NASA-Headquarters, for their encouragement during the course of this investigation.

ABSTRACT

The technique of differential thermal analysis (DTA), has been applied to the study of the Apollo 17 orange soil (74220,63) and the Apollo 16 glass coated anorthite (64455,21). These glasses have shown accentuated exotherms of strain relief in the annealing range which is indicative of rapid cooling. These have been amenable to interpretation by comparison to the known history of synthetic glasses. Synthetic glasses have been prepared whose similarity in behavior between the lunar glasses and their synthetic analogs is striking.

Approximate rates of cooling of the lunar glasses have been determined from comparative DTA of lunar and synthetic glasses and from the determination of the relation of strain relief in the annealing range to quench rate.

At higher temperatures the glasses show exotherms of crystallization. The crystallization products associated with the exothermic reactions have been identified by x-ray diffraction and the surface morphologies developed by strain relief and crystallization have been characterized with scanning electron microscopy.

The results have been discussed in view of the current lunar knowledge in this area. Some attempts have been made to apply this data to a geochemical interpretation of the origin of the 74220,63 and 64455,21 samples.

SECTION 1

INTRODUCTION

The fine fines, coarse fines, and rocks returned from the Apollo missions have an abundance of glass, as has been reported in the lunar science literature. Since glass is a noncrystalline, isotropic material, it does not readily lend itself to direct analysis by the standard methods of mineralogical characterization such as optical mineralogy, descriptive mineralogy and x-ray analysis. In view of this, the dynamic technique of differential thermal analysis (DTA), which is commonly used in glass-ceramic research, has been applied to the study of Apollo 16 and 17 glass-containing materials.

Differential thermal analysis is a technique which enables chemical reactions or phase transformations to be studied for substances of high temperature. It is a useful method for studying the annealing of glass, characterized by an endothermic (absorption of heat) reaction. This is followed by exotherms (heat evolution) of crystallization at higher temperatures. In contrast to the annealing endotherms of terrestrial tektites and commercial glasses, this study has revealed that the lunar glasses are characterized by accentuated exotherms of strain relief which are caused by rapid cooling.

Glasses of very similar composition to the lunar samples were synthesized in a reducing environment at various rates of cooling and their thermal history profiles obtained using DTA. The similarity in behavior between the lunar glasses and their synthetic analogs on a reproducible basis is striking. The lunar samples show evidence for strain in their structure which is amenable to interpretation by comparison to the known history of the synthetic glasses. This enables us to determine the relation of the strain relief exotherm to the cooling rate from which the glass originated.

Following the annealing exotherm, the synthetic and lunar glasses produced one or more exotherms of crystallization at higher temperatures. The thermal energy changes observed in the DTA profiles were related to the development of crystallinity by x-ray diffraction. The crystallization products associated with the exothermic reactions and higher temperature processing were identified up to 1200°C.

The surface morphologies and microstructure developed during the strain relief, crystallization, and high temperature reactions were characterized by scanning electron microscopy. This was accomplished by either direct observation of the topological developments with hot-stage scanning electron microscopy (SEM) or by examination of samples taken from DTA runs which were arrested following specific reactions or at specific temperatures.

The objective was correlation of the glass and crystallization morphologies and cooling rates to determine the thermal history of specific samples and formulate a geochemical interpretation of origin. The glasses studied were the Apollo 17 orange soil (74220, 63) and the glass coating (64455,21) of Apollo 16 64455 rock, an ovoid, rounded shocked anorthosite.

SECTION 2

EXPERIMENTAL TECHNIQUES AND PROCEDURES

2.1 SYNTHETIC LUNAR GLASS PREPARTION

Several synthetic glasses were prepared for investigation. The objective in using these materials was to enable sufficient quantities of material to be available for the performance of necessary experiments and related studies against which the behavior of actual lunar material could be compared. Lunar glasses are not available in sufficient quantity for this kind of study, and their true value may be best exploited by comparison of carefully selected experiments against a well-documented background of data from synthetic materials.

2.1.1 PREPARATION OF 64455,21 GLASSES

The composition of the first synthetic glass produced in this program was obtained by constructing a histogram from published data from lunar glasses obtained from earlier missions (before Apollo 16). A glass was made from this "average" composition (ignoring minor constituents) and melted and homogenized in a platinum crucible at 1400°C. Since lunar glasses are probably formed in non-oxidizing conditions, all glass-forming processes and heat treatments were performed in an inert argon atmosphere. Also, the iron oxide used in the formulation of the glasses was a mixed ferrous/ferric oxide so as to encourage a high level of ferrous iron in the melt.

It was observed that a high cooling rate was required in order to produce an amorphous glass from the compositions studied. Typically, a cooling rate of several degrees per second was required to avoid nucleation and growth of crystalline phases. The composition of the melt was determined and compared to that of an actual specimen of Apollo 16 glass (64455,21) using an electron probe x-ray microanalyzer (Cameca). As a result of comparing the relative response of the various elements in this side-by-side situation in the probe, modifications to the compositions were made in subsequent melts so as to obtain a closer match between synthetic and actual material. After three iterations a close match in composition was obtained between the lunar specimen and a snythetic melt SLG-4. The composition of synthetic glasses SLG-3 and SLG-4 used for most of the experiments discussed are shown in Table 1.

Table 1. Compositions of Synthetic Glasses SLG-3 and SLG-4

(Made for use in experiments to simulate the composition and thermal history of lunar sample 64455,21)

Oxide	SLG-3	SLG-4
SiO_2	46	47
Al_2O_3	25	25
CaO	10	12
MgO	12	10
FeO*	6	5
Na_2O	1	1

* Supplied as Ferrous/Ferric Oxide (Fisher I-119)

2.1.2 PREPARATION OF 74220,63 GLASSES

Glass composition SLG-17 was formulated based on the orange soil analysis (74220,3) reported by the Preliminary Examination Team (PET)[1]. The published analysis and the synthetic glass composition are shown in Table 2. The glass was prepared in argon at 1400°C.

Glass composition SLG-17M closely approximates the DTA profile of the 74220,63 lunar material, as shown in Table 2.

2.2 DIFFERENTIAL THERMAL ANALYSIS

2.2.1 PRINCIPLE OF OPERATION

Differential thermal analysis (DTA) techniques were used to study the behavior of lunar and synthetic glasses when they were reheated under controlled conditions. Differential thermal analysis is a technique that measures the temperature difference between a sample and reference material such as alumina having a simple linear behavior as each is heated at uniform rates (such as at 10°C/min) through the same temperature range. It is a heat-averaging

Table 2. Composition of 74220,3 Compared With SLG-17 and SLG-17M

Composition of lunar material 74220,3 as determined in other investigations, and the composition of the synthetic glasses SLG-17 and SLG-17M made for comparative purposes in the experiments described.

Oxide	74220,3 (1)	SLG-17	SLG-17M
SiO_2	38.57	38.6	38.6
TiO_2	8.81	8.81	8.81
Al_2O_3	6.32	6.32	5.50
FeO	22.04	-	-
FeO/Fe_2O_3	--	22.04	22.20
MnO	0.30	-	-
MnO_2	--	0.37	0.32
MgO	14.44	14.44	14.44
CaO	7.68	7.68	7.13
Na_2O	0.36	0.36	0.51
K_2O	0.09	0.09	-
P_2O_5	0.04	0.04	-
S	0.07	0.07	-
Cr_2O_3	--	-	0.52

Note: Raw material used to formulate SLG-17 and SLG-17M include wollastonite, spinel, magnesium sulfate, aluminum phosphase, manganese dioxide, sodium and potassium carbonates, as well as the oxides of silicon, titanium, magnesium, and chromium.

(1) Summary of Apollo 17 Preliminary Team Results, Compiled by W. C. Phenney, March 5, 1973.

technique and reflects the absorption or evolution of heat over a finite time span, which is determined by the sample geometry, heating rate and thermal contact of the sample with the thermocouple sensor.

A sample of the lunar glass and a powdered reference sample which shows no heat effects in the temperature range of interest are both heated in a suitable furnace. Each of the powdered samples is packed around a thermocouple junction. The differential voltage readings of the two couples plotted against temperature, as the general temperature of the furnace is increased, indicates any heat absorption or evolution in the lunar sample. The net emf representing the temperature difference between the sample and inert reference is plotted as the ordinate against the reference sample temperature as the abscissa.

In the absence of enthalpic change during heating or cooling the temperature difference between sample and reference is constant and, therefore, the net output is constant. This yields a level baseline. During the reaction, the rate of change deviates from that of the inert reference material.

For the case of an endothermic reaction, an increase in heat content is required to accomplish the transformation. The temperature of the sample tends to remain constant while the heat required to complete the phase transformation is absorbed by the sample. Once the transformation is completed, the sample will heat at a faster rate until the temperature difference between it and the reference is minimized. At this point, the substance resumes heating at the programmed rate.

2.2.2 GLASS PROFILE SCHEMATIC AND EXPLANATION

A schematic of the DTA profile of a typical glass is shown in Figure 1. The features of the three principal regions are illustrated. These include annealing (low temperature range), crystallization (middle temperature range), and melting of the crystallized phases (high temperature range).

As the temperature of the glass is increased above ambient, a dip is observed in the DTA curve when the annealing point is reached. The start of the endotherm at A is the transition temperature at which the solid glass begins to transform into a viscous liquid. Point B is the softening point where the glass begins to soften under its own weight. The AB section of the profile identifies the transformation range of the glass.

With further increase in temperature, one or more exothermic peaks such as GE are observed corresponding to the precipitation of one or more crystalline phases. The endotherm EG is the melting endotherm of the crystalline phase D.

The intensity of the endothermic peak varies with the degree of annealing as shown in Figure 2. Slower cooling from the molten liquid state will show an increase in the endothermic effect. Rapid cooling, however, accentuates an exothermic peak[2]. This is because rapidly cooled glass has a high fictive temperature. That is, the high temperature structure is "frozen-in" which creates a nonequilibrium strain state in the glass at room temperature[3].

In this study the differences in the annealing effect of lunar glass as a function of relative cooling rate were investigated with DTA by:

1. Determining the quench rate at which the strain-relief exotherm originated in lunar glass by successive quenching and reheating; and
2. Matching the annealing exotherms of synthetic glasses quenched at known cooling rates to that of the lunar glass.

2.2.3 TECHNIQUES

The glasses were investigated using a DuPont Model 990 DTA unit with separate cell modules covering the ranges from room temperature to 850°C or to 1200°C.

Most compositions studied were formed by melting batches at 1400°C; and, therefore, a complete DTA profile was possible up to 1200°C in most cases without any melting. Using the 1200°C cell module profiles of the complete strain relief, softening, nucleation, and crystal growth behavior of the glasses were obtained. This cell employed platinum sample cups with thermocouples external to the cups. This arrangement was essential for studies of the devitrification of most of the glasses used in this work: crystallization typically

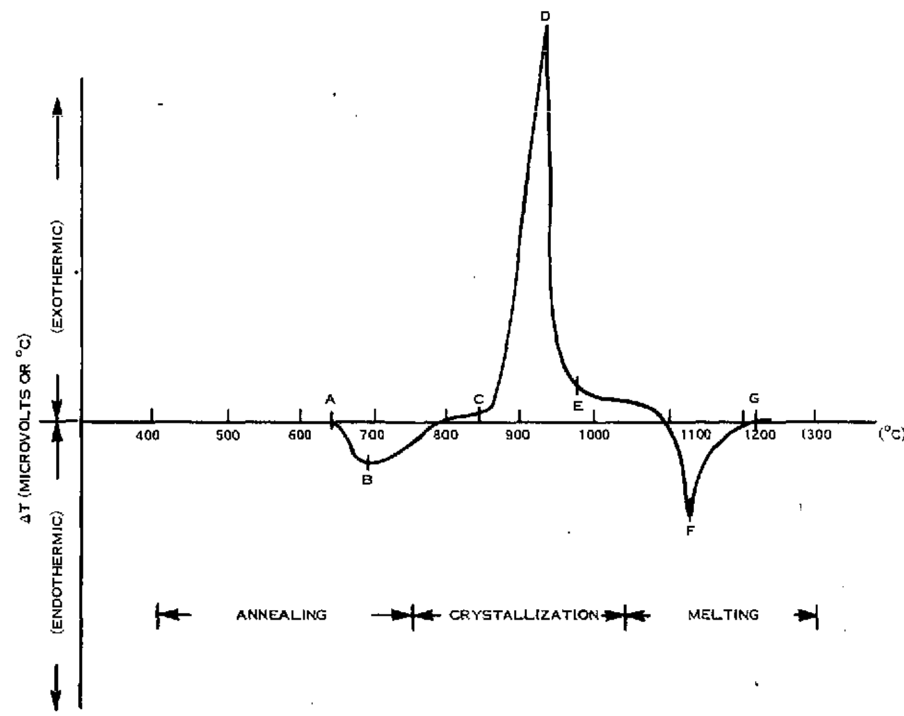

Figure 1. Schematic DTA Profile of a Typical Glass Showing the Annealing, Crystallization and Melting Regions

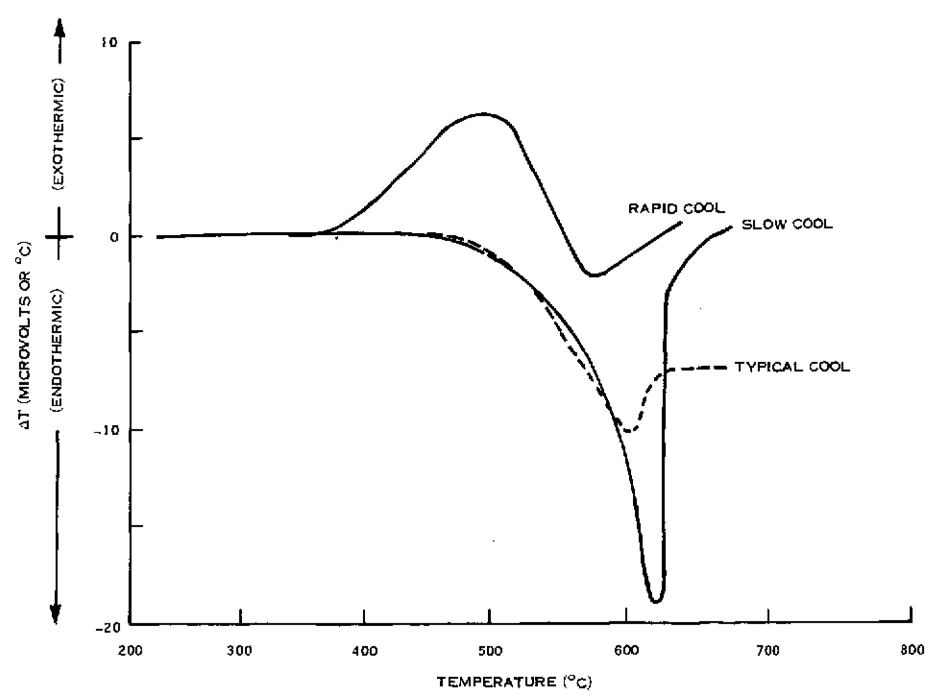

Figure 2. Schematic of the Changes Observed in the DTA Profiles of Glass as a Result of Differences in Quench Rate. Lunar Glass has the Accentuated Exotherm of Rapid Cool.

occurred at 850-950°C. However, for maximum sensitivity and study of the strain-relief exotherms in the glasses, the low temperature module (with the thermocouple embedded in the specimen) was used. Strain relief between 500°C and 750°C was observed in most glasses used, depending on prior thermal history.

To conserve lunar glass, a standard specimen size of 10 mg of -270 mesh powder was employed and was held in a fused silica vial for the low temperature module with a chromel/alumel thermocouple immersed in the center of the specimen. All DTA experiments were performed in an argon atmosphere to relate to the non-oxidizing lunar thermal environment. Standard heating conditions of 10°C/minute were employed. For some experiments, controlled cooling rates from particular temperatures were imposed on glass specimens within the DTA apparatus itself so that a subsequent DTA run would indicate the amount of strain introduced by this controlled cooling. It was, of course, possible to completely anneal specimens within the DTA itself by slow cooling so that a subsequent run showed no evidence for internal strain in the glass.

2.3 QUENCHING EXPERIMENTS

2.3.1 TECHNIQUES

Controlled cooling rates from particular temperatures in the annealing range were imposed on glass specimens within the DTA cell itself, so that a subsequent DTA run would indicate the amount of strain introduced by this controlled cooling.

High quench rates were not possible in the DTA cell, so a facility was constructed where powdered glass specimens could be given controlled heat treatments in argon, and the cooling ranges could be documented. This apparatus consisted of a small platinum boat on the end of a fused silica tube that could be introduced or withdrawn from a tube furnace at controlled rates manually or using a mechanical drive. Specimen temperature was recorded by a platinum/platinum-10% rhodium thermocouple welded directly to the base of the specimen boat. The furnace was set at the desired temperature, using a flowing argon atmosphere, and the specimen temperature and the time were recorded automatically on a strip chart recorder so that accurate determinations of the specimen thermal history could be made. The exposed end of the muffle tube was water-cooled to enable rapid quenching of glasses from the melt.

This apparatus was employed for controlled quenching of glass melts and of the powdered glasses after annealing at appropriate temperatures. Specimens of 2-3 gms of raw batch, or down to only 10 mg of powdered glass, could be treated in this manner. The time-temperature profile of a typical quench from the melt exemplified by SLG-17M, is shown in Figure 3A. A time-temperature profile of a quench from the annealing range is shown in Figure 3B.

2.3.2 SIGNIFICANCE OF QUENCH RATES OF SYNTHETIC GLASSES

The quenching of the melt compositions enables the glass structure to be obtained in a metastable condition at room temperature. As a result of this quenching, a state of strain exists in the glass which can be relieved on subsequent heating. An indication of the previous thermal history of the glass can thus be obtained by a study of the amount of strain built into the structure as a result of continued rapid quenching below the fictive temperature. The release of this strain energy as the glasses are reheated may be detected and measured quantitatively by careful differential thermal analysis (DTA) studies as the glasses are reheated under controlled conditions. Major emphasis has been placed on the determination of strains associated with quenching from the annealing range of the glass, i.e., in the region slightly above the fictive temperature of the initial quenching but below the temperature for crystal nucleation in the particular composition studied.

A wide range of quench rates and associated strain determinations can be employed in glasses quenched from this temperature range. An indication of the previous thermal history of the glass can also be obtained by a study of the tendency of the melt to devitrify as the quench rate from the melt is reduced. However, in quenching from the melt, only rapid rates can be used or devitrification of the melt takes place. There is thus a minimum quench rate for any given composition from the melt below which devitrification would occur, and an amorphous glass structure could not be attained at room temperature.

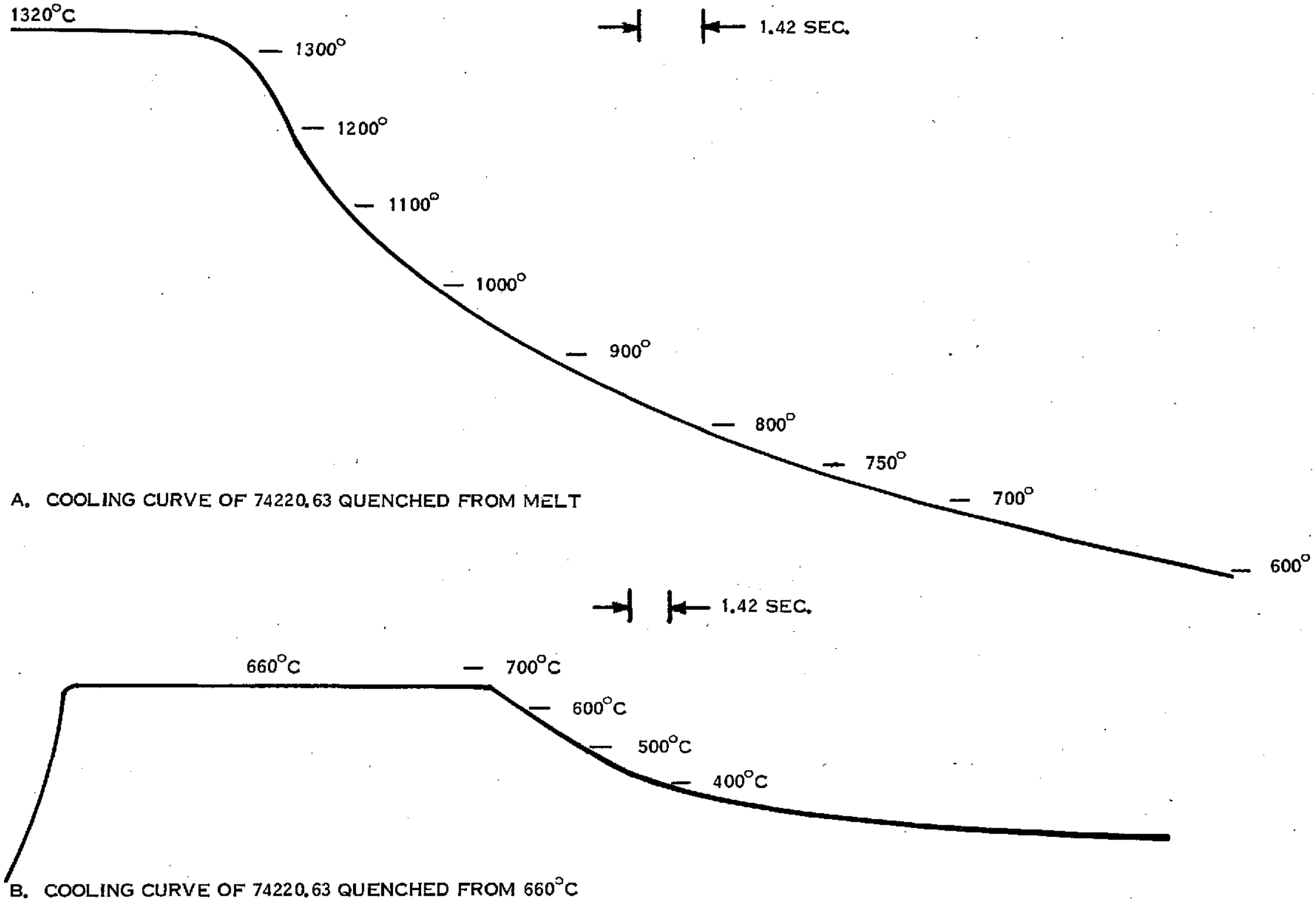

Figure 3. Typical Cooling Curves From (A) the Melt and (B) the Annealing Range

Similarly, there is a minimum quench rate from the annealing range below which no strain is introduced and a fully annealed glass structure results. The data obtained from this work can, therefore, at least indicate a minimum value of quench rate in either of these temperature regimes. While the average cooling rate from the melt should be higher than the rate in the region of the glass transition, they should be of the same order of magnitude. The possibility of quantitative indications of quench rate above these minima has been explored in this program.

2.4 SCANNING ELECTRON MICROSCOPY

Scanning electron microscopy (SEM) was performed on samples 64455,21 and 74220,63 prior to heat treatment and at elevated temperatures. The objective was to determine the morphological changes associated with reactions of the glass as determined by differential thermal analysis. The analyses were conducted on a Cambridge Model S-4 Scanning Electron Microscope. Standard procedure was to carry out an energy dispersive x-ray analysis, i.e., EDX, of the exterior of the surface of each sample and morphological feature examined for identification of the elements present. An eyeball assignment was made for each element as to whether it was present in major, minor or trace proportions.

2.4.1 SAMPLE 74220,63 - PREPARATION AND IDENTIFICATION

Samples of the "as received" orange soil were mounted in polyvinyl acetate on a stainless steel stub following the procedure developed for this purpose by McKay and Laydle[4].

To examine the surface morphology associated with the strain-relief exotherm, the crystallization exotherm and higher temperature sintering of the 74220,63 particulates, DTA runs were made using the standard procedure established for this program. Runs were taken to 685°, 860°, and $1120^{\circ}C$, and the reactions arrested at temperature. The samples were cooled at $10^{\circ}C$ per minute in argon to room temperature, removed and mounted in the polyvinyl acetate on SEM stubs. The samples and studs were carbon coated.

Each sample was oriented in the SEM with color photomicrographs taken under a metallurgical microscope. Using this technique the color of each particle could be correlated with the SEM results.

2.4.2 SAMPLE 64455,21 - HOT-STAGE SEM TO 1000°C

A sample of the glass coating was mounted in a hot stage which was constructed to observe surface changes on 64455,21 in the SEM. The hot stage consisted of a rhenium boat with a platinum/platinum-10% rhodium thermocouple welded to the bottom. The boat and sample were placed in a vacuum evaporator and carbon-coated.

2.5 X-RAY DIFFRACTION

An attempt to identify which, if any, crystalline phases might be present in the lunar samples, and to perhaps relate thermal energy changes observed in DTA to the development of crystallinity, was an objective of the x-ray diffraction studies carried out in the lunar materials. Where appropriate, samples to be studied by the Debye-Scherrer powder x-ray diffraction technique were heat-treated in an argon atmosphere in the DTA cell at the appropriate temperatures for varying durations. These samples were used for SEM analysis so that any one sample would be well characterized.

SECTION 3

RESULTS AND DISCUSSION

3.1 SAMPLE 64455, 21

Results obtained from comparative DTA studies of synthetic glasses and on specimens of lunar glasses from the Apollo 16 mission are shown in Figure 4.

The total DTA profile (annealing and crystallization) for the synthetic glasses SLG-3 and SLG-4, after quenching from the melt, are shown in Figures 4A and 4B. There is a similarity in the profiles despite differences in composition (Table 1 Section 2.1.1). While the accentuated exotherms of annealing can be superpositioned, the crystallization exotherm of SLG-3 is about 50°C higher than that of SLG-4. SLG-3 also has a minor exotherm at 1040°C.

A detailed study of the relationship of the strain-relief exotherm to the quench rate from which the strain originated, is illustrated in Figure 5 for glass SLG-4. Figure 5A represents the strain from a sample quenched from the melt at approximately 3°C/second (see the total profile in Figure 4B and 4C). The removal of this strain by annealing at 700°C (i.e., the "peak" of the strain-relief regime indicated in Figure 5A) is shown in Figure 5B as an essentially flat profile (no exothermic activity). The sample shown in Figure 5B was cooled at a rate of 0.13°C/second after annealing prior to the DTA run.

To extent to which strain can be reintroduced into the glass by rapidly cooling from the annealing range is illustrated in Figures 5C and 5D. These data were obtained by quenching from 700°C (the annealing temperature) at rates of .4°C/second, for 5C, and 11°C/second for 5D. It may be seen that a strain equivalent to that introduced by quenching from the melt was introduced in this case by quenching from the annealing range.

A significant indication of the thermal history in the annealing temperature range, where the glass has relatively low viscosity, may be obtained by considering the degree of crystallization observed. Amorphous glass may only be obtained in these melts when cooled at least at a rate of several degrees per second. Therefore, as mentioned previously, there is a

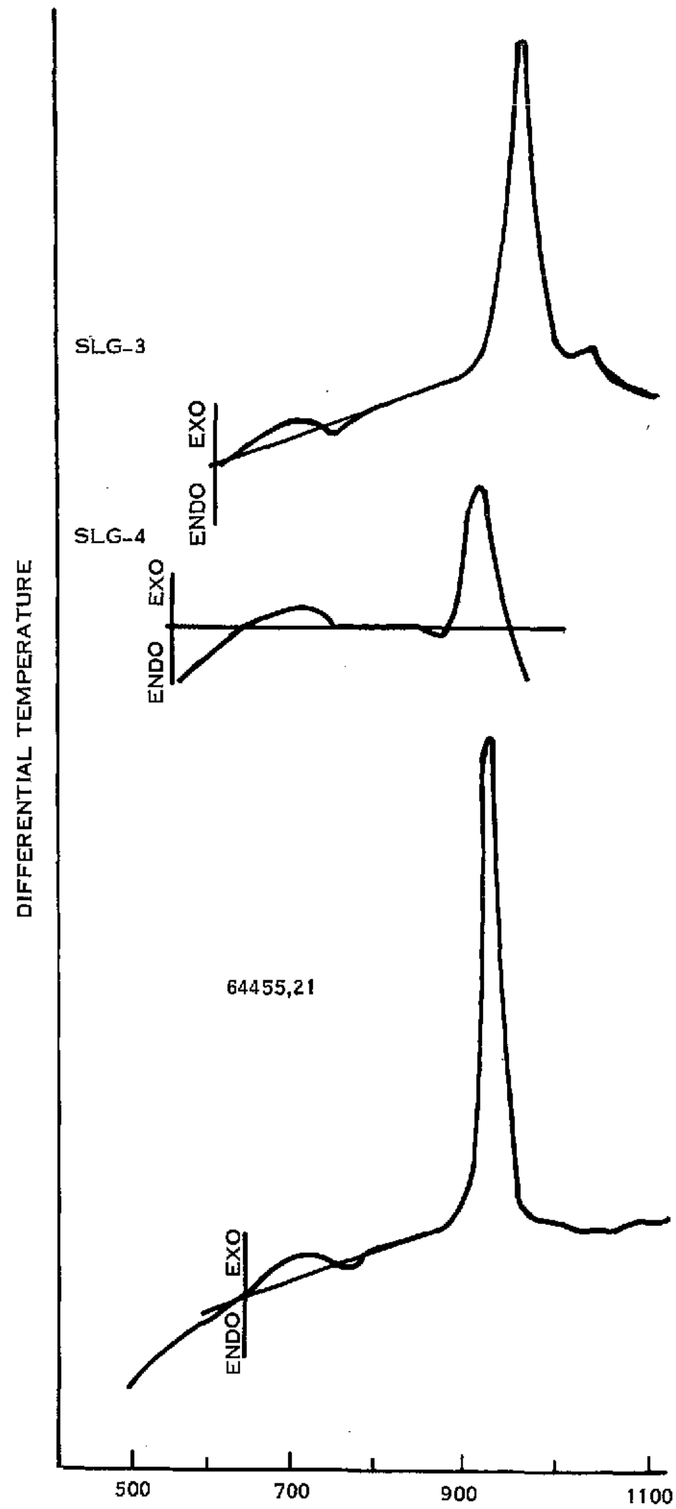

Figure 4. DTA Profiles of (A) Synthetic Glass SLG-3, (B) Synthetic Glass SLG-4, and (C) the 64455,21 Glass Coating. SLG-4 and 6445,21 are Similar in Composition and DTA Profile

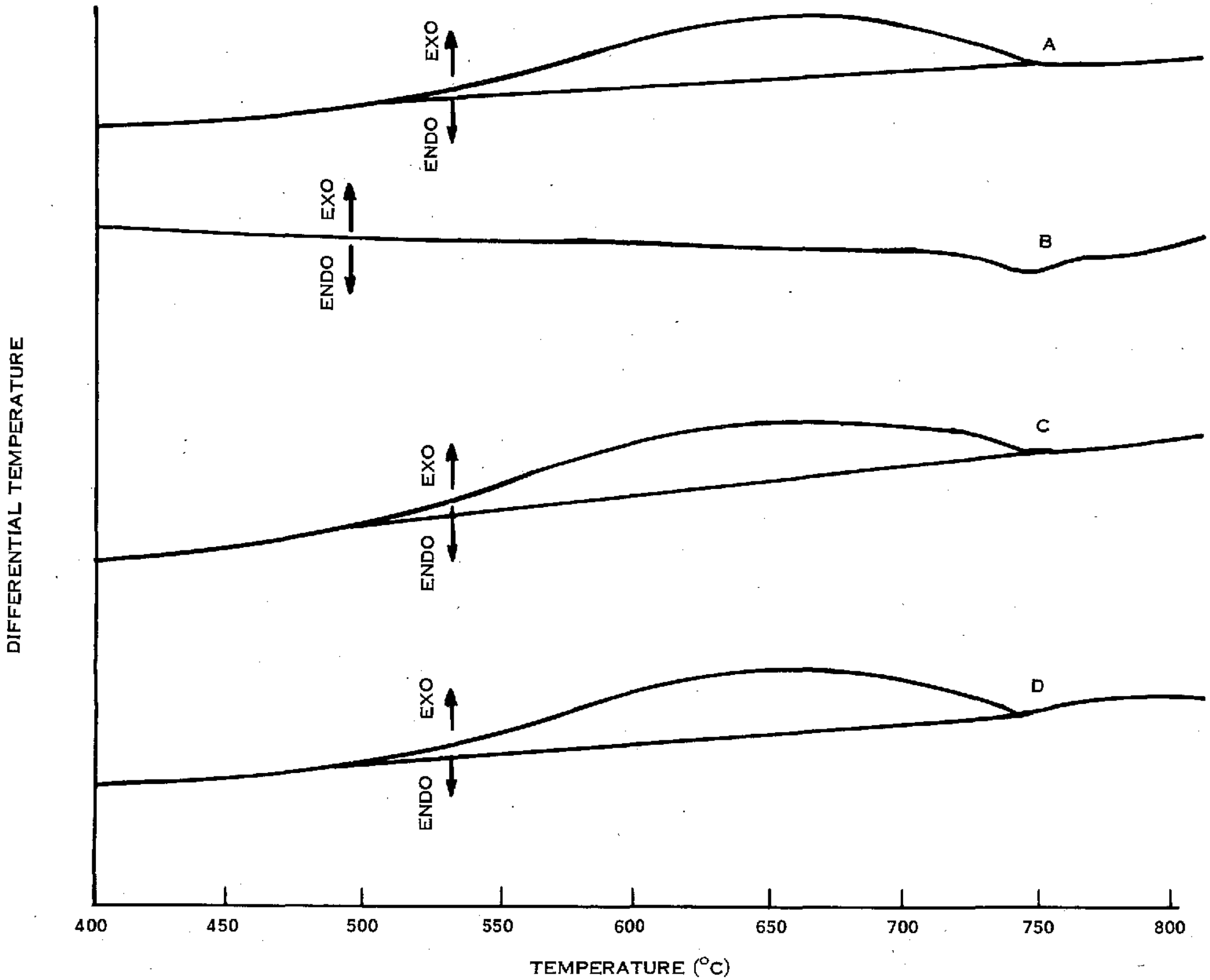

Figure 5. Details of the Strain Exotherm From DTA Profiles of SLG-4 Glass for Different Thermal Histories; (A) Quenched From the Melt at 3°C/Second; (B) Cooled From 700°C at 0.13°C/Second; (C) Cooled From 700°C at 0.4°C/Second and' (D) Cooled From 700°C at 11°C/Second

mimimum cooling rate from the melt in order to produce a glass from a particular composition (in these cases 2 to $10^{o}C$/second). Cooling rates higher than this may not be detected by these techniques; slower rates result in development of crystalline phases in amounts inversely proportional to the cooling rate.

Similarly there is a mimimum cooling rate below which no strain is introduced in the glass (essentially a fully annealed structure; in the case of SLG-4 this rate appears to be about $0.2^{o}C$/second). For cooling rates higher than this, a proportionate amount of strain is introduced into the structure and may be detected by DTA. There appears to be a maximum amount of strain that can be built into this particular structure such that once again higher quench rates do not produce detectable changes in the glass (as measured on -270 mesh powder).

The glass coating from the Apollo 16 lunar sample along with the synthetic glass SLG-4, following a $1200^{o}C$ anneal in the DTA cell, were studied by means of the Debye-Scherrer powder x-ray diffraction technique. The appropriate data are presented in Table 3.

The overall agreement of "d" spacing values for the respective samples is good. There are however several lines ("d" values of 8.3, 4.9, 2.84, 2.42, 1.80, 1.68 and 1.58 Å) exclusive to the lunar glass. The best fit for the diffraction patterns of both the lunar glass and SLG-4 is any one of the several plagioclase fedspar minerals, which include the end members anorthite and albite as well as the intermediates, bytownite, labradorite, oligoclase and andesine. According to microprobe analysis the lunar glass is substantially richer in CaO, 13.6%, than in Na_2O, only .4% being present [5]. This would narrow the choice of plagioclase minerals to either bytownite, of composition close to 0.77 $CaAl_2Si_2O_8$-0.23 $NaAlSi_3O_8$, or anorthite which is $CaAl_2Si_2O_8$. Since both materials have the same triclinic structure with very similar lattice spacings, any small differences that exist are of no consequence when comparing diffraction patterns. The bytownite diffraction pattern was arbitrarily selected and is presented in Table 3.

Table 3. Comparison of X-ray Diffraction Data for 1200°C Crystallized Apollo 16 Glass Coating (64455, 21) and SLG-4

64455, 21		SLG-4		20-528A, 9-467 (ASTM Card No.) Bytownite	
d Å	I/I_o	d Å	I/I_o	d Å	I/I_o
		8.3	VVVW		
				6.50	9
6.45	VW	6.4	VVW	6.42	9
				5.81	10
		4.9	W		
4.70	VW	4.6	W	4.69	50
4.05	M	4.05	M	4.04	100
3.78	M			3.77	29
		3.74	W	3.76	37
3.68	M	3.60	W	3.63	23
3.48	VW			3.46	50
3.42	VW			3.41	40
3.36	VW	3.36	MW	3.36	8
				3.25	29
				3.21	84
(VB) 3.20	VS			3.20	86
		(VB) 3.18	VS	3.18	86
				3.13	23
		3.00	M	3.04	12
2.95	M			2.95	17
				2.94	16
(B) 2.90	W	2,90	M	2.91	7
		2.84	M		
2.65	W	2.63	MW		
(B) 2.51	S	(B) 2.51	MS	2.51	19
				2.50	9
				2.47	8
				2.46	13
		2.42	M	2.39	9
		2.32	VVW	2.37	13
2.28	VW	2.24	VVW		
2.14	W	2.16		2.14	24
2.08	W	2.09	W		
2.01	W	2.02	W		
1.93	W	1.94	VW		
1.89	VW	1.88	W		
1.84	M	1.83	MW		
		1.80	W		
1.76	M	1.76	W		
		1.68	M		
(B) 1.61	M	1.63	W		
		1.58	W		
		1.56	MW		
(B) 1.48	M				
1.43	VW	1.43	M		
1.39	VW				
1.36	W				

The close correspondence that exists between the diffraction data for bytownite and the Apollo 16 lunar glass in particular is evident. The major discrepancies include absences of weak lines ("d" values of 6.50, 5.81, 2.39 and 2.37 Å), as well as several strong lines in the vicinity of 3.20 Å, 2.95 Å and 2.51 Å. The missing weak lines probably reflect a state of somewhat reduced crystallinity existing in the lunar glass while the strong lines are undoubtedly present but not resolved in the photographs, as evidenced by pronounced broadening of lines having "d" values of 3.20 Å, 2.90 Å and 2.51 Å. The patterns for bytownite as obtained from the ASTM file do not extend beyond the lower limit of "d" spacing value 2.14 Å, making it necessary to refer to data for other plagioclase minerals such as anorthite and oligoclase in this range. The agreement for smaller "d" spacing values is also found to be quite good. The somewhat poorer agreement that is found when comparing SLG-4 and bytownite diffraction data suggests a slight compositional variation.

The sample for high temperature examination was mounted in the boat in the SEM as shown in Figure 6A. With heating a change in surface morphology was observed between 960° and 975°C. This structural change can be correlated with the DTA exotherm of crystallization which is completed by 975°C (Figure 4C).

Figure 6B and 6C are room temperature photographs comparing the original glass surface and a freshly fractured edge before placement in the boat with the surface structure after heat treatment to 1000°C. Note that a convoluted, ropy structure has developed on the original and fractured (Figure 6F) surface. Micromounds on the original glass surface appear to have partially deformed and crystallized. The original surface also shows softening and deformation.

Figure 6D is a view at 460°C of a banding effect whose contrast increased markedly over that a room temperature. The interpretation is not certain but the bands may comprise regions of different electrical conductivity, which would affect their beam charging properties. Electrical conductivity of these oxides increases with increasing temperature[6], whereas the secondary electron emission ratio is essentially temperature independent[7].

Figure 6E shows the structure change between 960° and $975^{\circ}C$ at temperatures in the hot stage.

Picture contrast changed noticeably as the sample was heated. Contrast first increased around 300° -$400^{\circ}C$ (Figure 6D), then slowly decreased at about $600^{\circ}C$. Above $800^{\circ}C$ the picture washed out very readily, requiring large increases in video black level. A line-of-sight opaque shield between the boat and detector did not significantly improve contrast. A metal grid (about 70% transparent) between the boat and the detector did improve contrast up to $1200^{\circ}C$ when biased about 5 volts negative with respect to the boat. It was concluded from this that thermionic electrons were the most important source of white noise at these temperatures.

To examine changes in the surface morphology of the 64455, 21 surface above $1000^{\circ}C$, small specimens of the glass placed in platinum boats were heat treated at $1200^{\circ}C$ and $1300^{\circ}C$ for ten minutes in argon in an externally wound tube furnace. After quenching in argon, the samples were mounted on stubs and carbon coated.

The recrystallized glass surface at $1200^{\circ}C$ is characterized by "flower-shaped" or "splash-like features" and spherical particles embedded in the surface (Figure 7A). Energy dispersed analysis of the "splash-like" feature has Si, Ca and Al present in major proportions, Fe and Mg in minor proportions and Cr in a trace amount. In contrast, the adjacent spheres, shown in Figure 7B, have Fe and Ni in major proportions and Si, Ca, Al and Cr in trace amounts. The Si, Ca, Al and Cr must likely exist on the coating on the spheres, which is shown in Figure 7B.

Figure 7C shows a high magnification micrograph of the sample fired at $1300^{\circ}C$. The "flower-design" developing at $1200^{\circ}C$ may be the initiation of the surface morphology which is dominant at $1300^{\circ}C$.

Figure 6. Hot State Scanning Electron Microscopy of 64455, 21 Glass Coating to 1000°C. (A) Glass Coating Mounted in Boat in SEM Showing the Study Surface; (B) Room Temperature View of the Glass Surface Before Heat Treatment (2700X); (C) Room Temperature View After Heat Treatment to 1000°C (2600X); (D) Shows a Banding Effect During Heating at 460°C in the SEM; (E) Shows the Structural Change Between 960° and 975°C at Temperature in the Hot Stage; (F) Shows the Convoluted, Ropy Structure Which Has Developed on the Original and Fractured Surface.

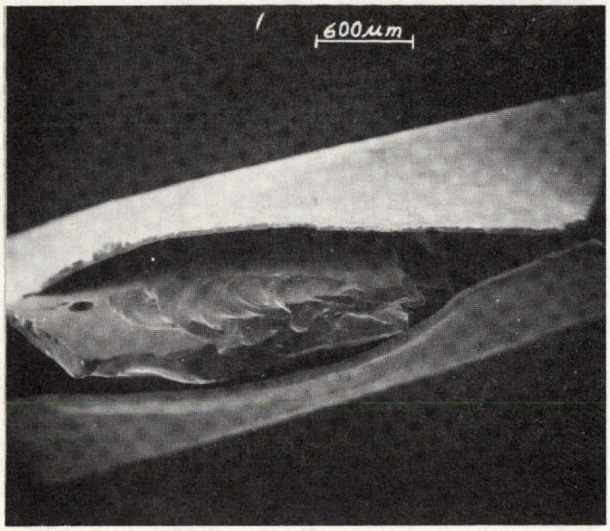

A

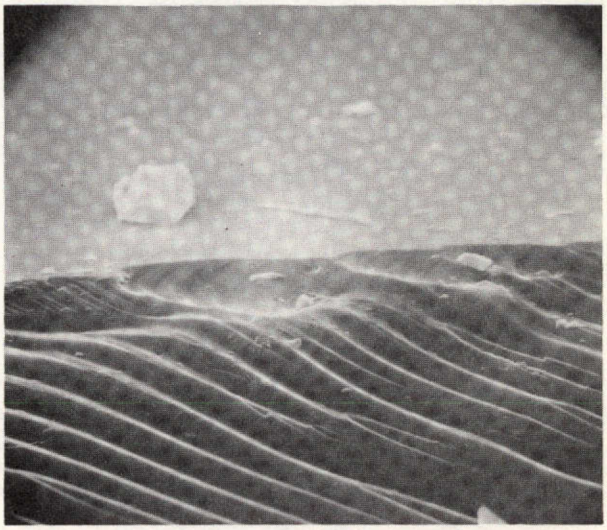

B

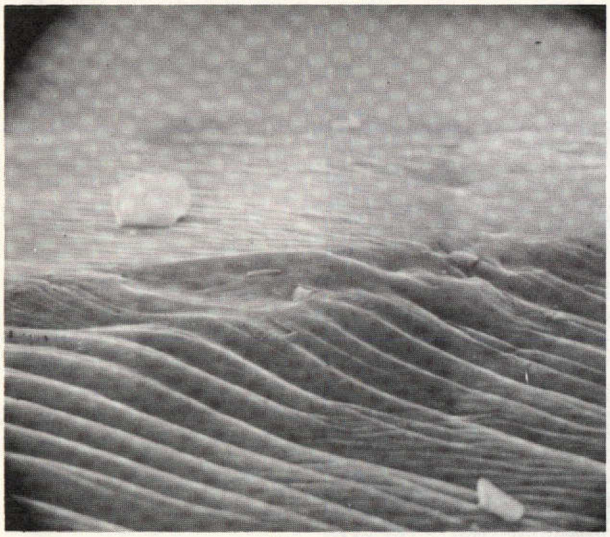

C

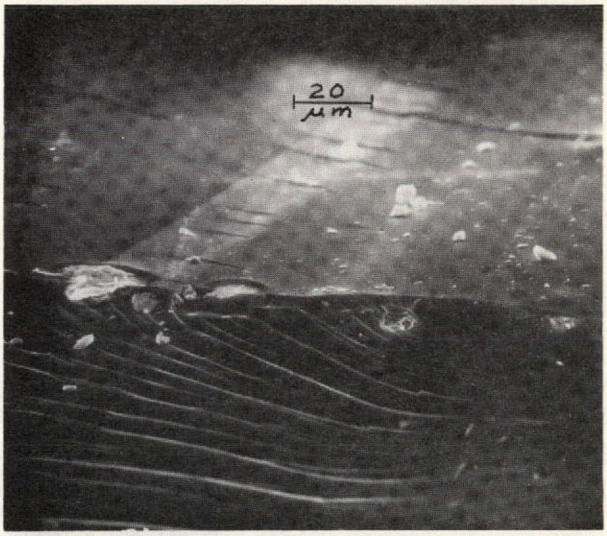

D

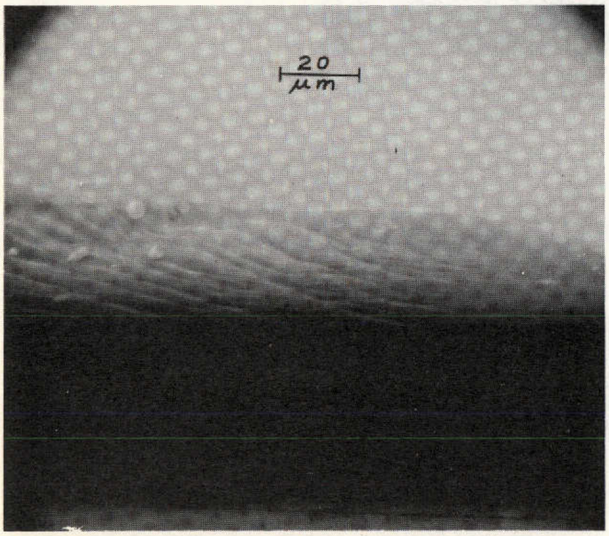

E

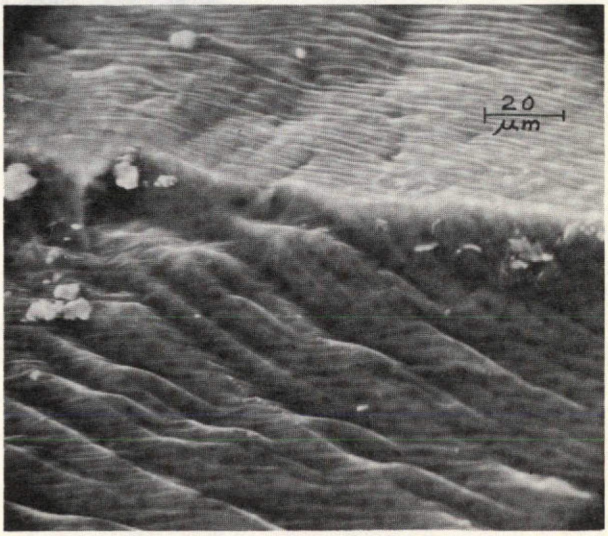

F

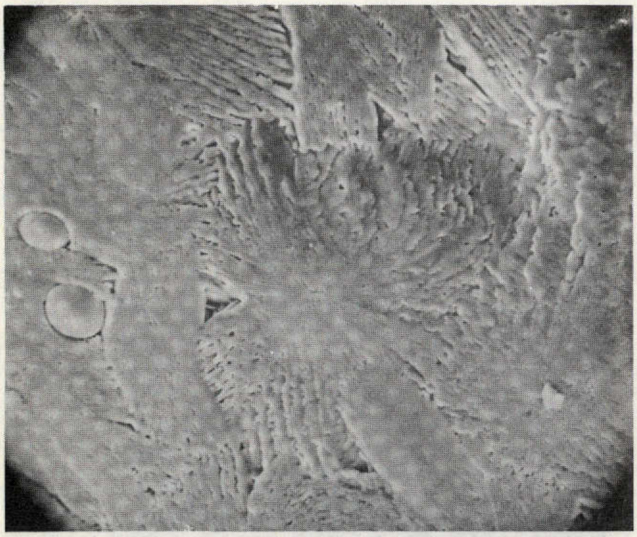

A

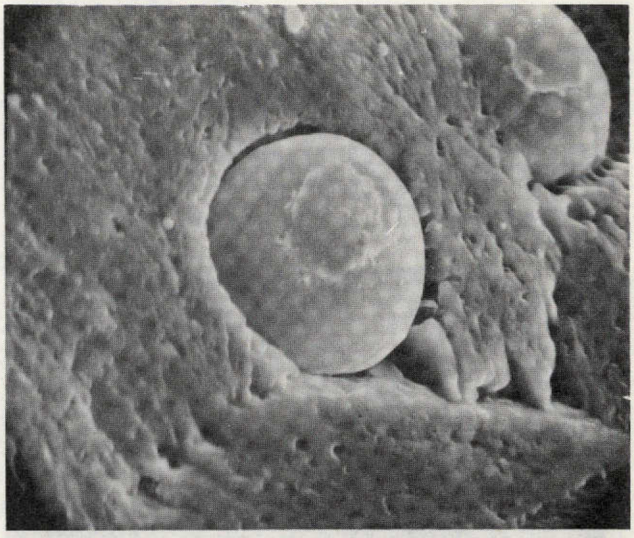

B

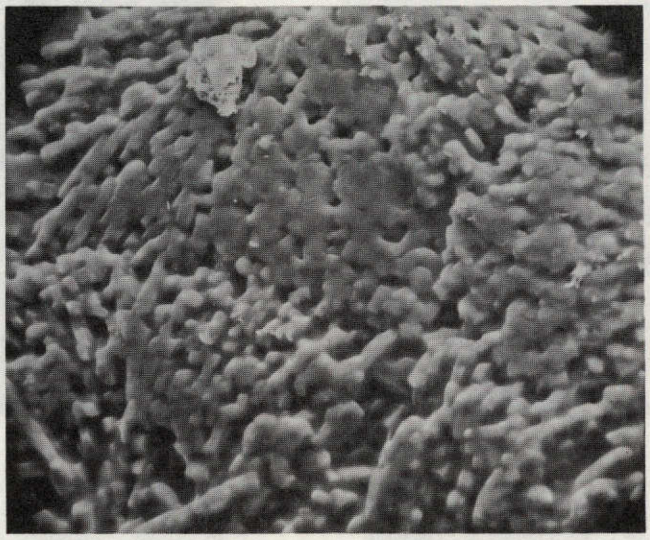

C

Figure 7. High Temperature Morphologies in the Recrystallized 64455,21 Glass Surface. (A) Shows "Flower-Shpaed" or "Splash-Like Features" and Spherical Particles Embedded in the Surface Recrystallized at 1200^{o}C (500x); (B) The Embedded Ni-Fe Spheres Showing a Surface Coating at 2200x; (C) Morphology of the Surface Crystallized at 1300^{o}C

3.2 SAMPLE 74220, 63

The DTA profile of 74220, 63 is shown in Figure 8. It shows the accentuated exotherm of strain relief which is characteristic of rapid cooling.

It is fortunate that the lunar samples studied show evidence for strain in their structure which is amenable to interpretation by comparison to the known history of the synthetic glasses. The similarity in behavior between the lunar glasses and their synthetic analogs is striking. The DTA profile for synthetic glass SLG-17 which was based on the composition of 74220, 3 (Table 2) is shown in Figure 8A. A striking similarity may be noted between the actual lunar specimen 74220, 63 and the SLG-17 composition which was quenched from the melt at 8^{o}C per second.

Even more striking is the similarity between SLG-17M when formed by quenching at 45^{o}C per second and the 74220, 63 profile. This is shown in Figure 8. Synthetic glass SLG-17M contains the small exotherm at 740^{o} -750^{o}C which was absent in SLG-17.

A detailed study of the relationship of the strain-relief exotherm to the quench rate from which the strain originated was conducted on the synthetic SLG-17M and the lunar 74220, 63 glass. The SLG-17M results are shown in Figure 9. Figure 9A represents the strain from a sample quenched from the melt at approximately 45^{o}C per second (see the total profile in Figure 8). This specimen was cooled from 660^{o}C at 0.08^{o}C per second. As shown in Figure 9 the strain was removed. Strain was then reintroduced when the glass was cooled from 660^{o}C at 0.4^{o}/second and reheated (Figure 9D).

The strain-relief experiments were reproduced with the 74220, 63 glass (Figure 10). Figure 10A represents the strain in the "as received" samples. Based on the strain-relief exotherm induced in synthetic glasses quenched from the melt, the rate of cooling of this sample was in the vicinity of 45^{o}C per second. This glass was cooled from 660^{o}C at 0.1^{o} per second and, upon reheating, the strain was removed (Figure 10B). The glass was then cooled from 660^{o}C at 0.33^{o}C per second and the strain was re-introduced (Figure 10C). Quenching of the sample from 660^{o}C at 48^{o} per second (Figure 10D) induced a strain exotherm which appeared to be similar in magnitude to that induced when the glass was quenched from the melt (Figure 10A).

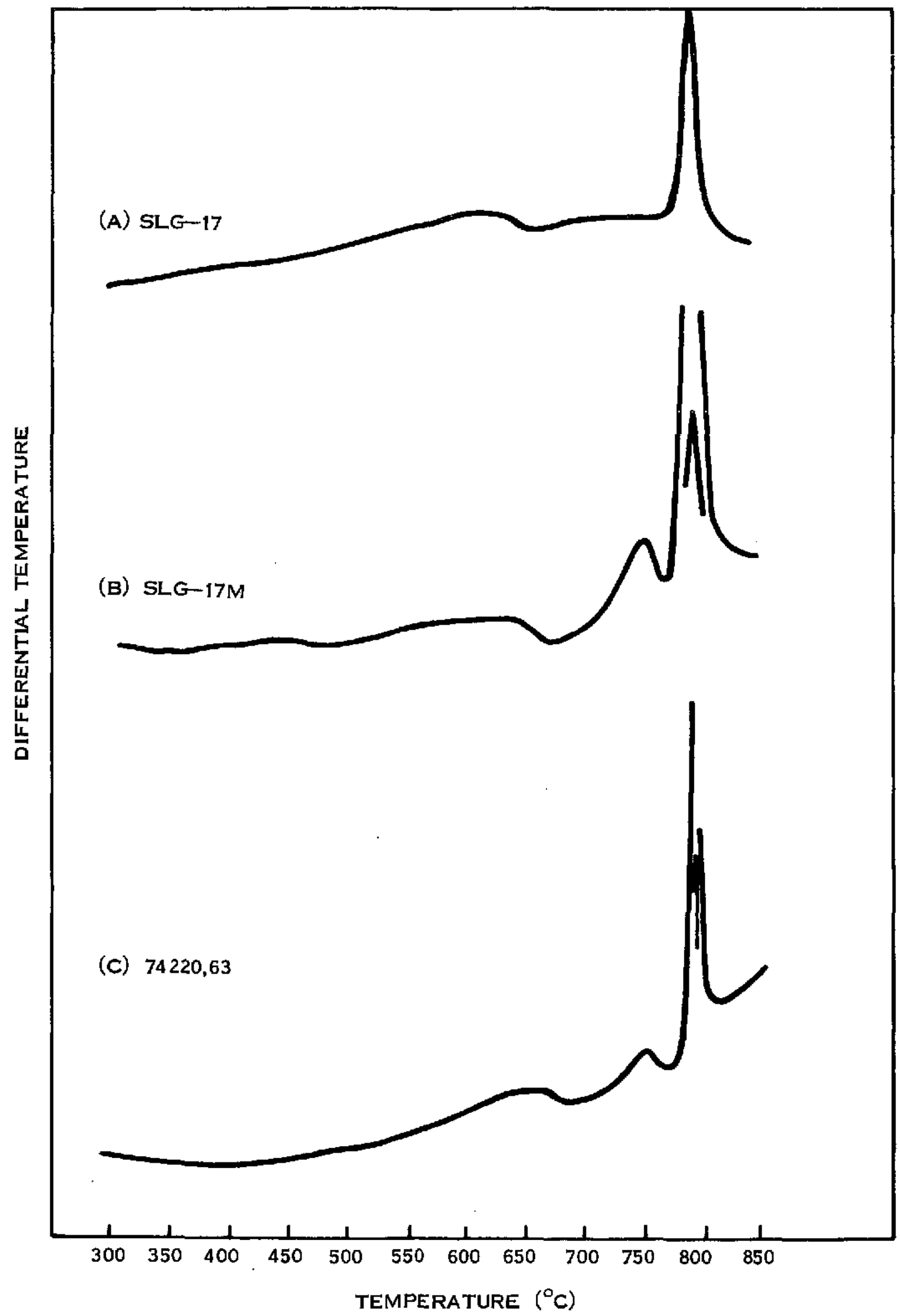

Figure 8. DTA Profiles of the Lunar and Synthetic 74220,63 Glass. (A) is the Profile of Synthetic SLG-17 Quenched at 8°C per Second; (B) is Synthetic SLG-17M Quenched at 45°C per Second; (C) is the Lunar Glass 74220,63.

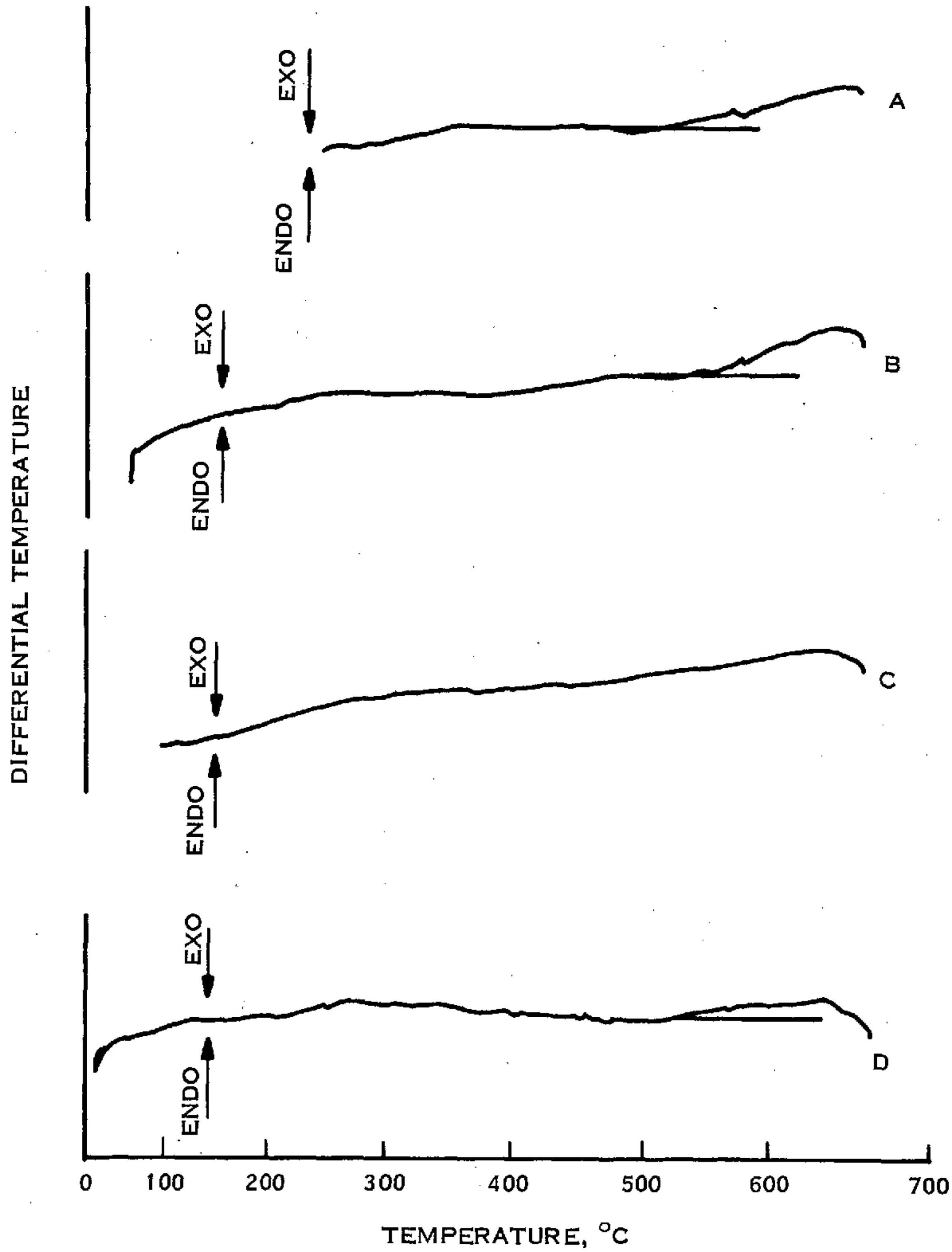

Figure 9. Details of the SLG-17M Glass for Different Thermal Histories: (A) Quenched From the Melt at 45°C per Second; (B) Cooled From 660°C at 0.33°C per Second; (C) Cooled From 660°C at 0.08°C per Second; (D) Cooled From 660°C at 0.41°C per Second.

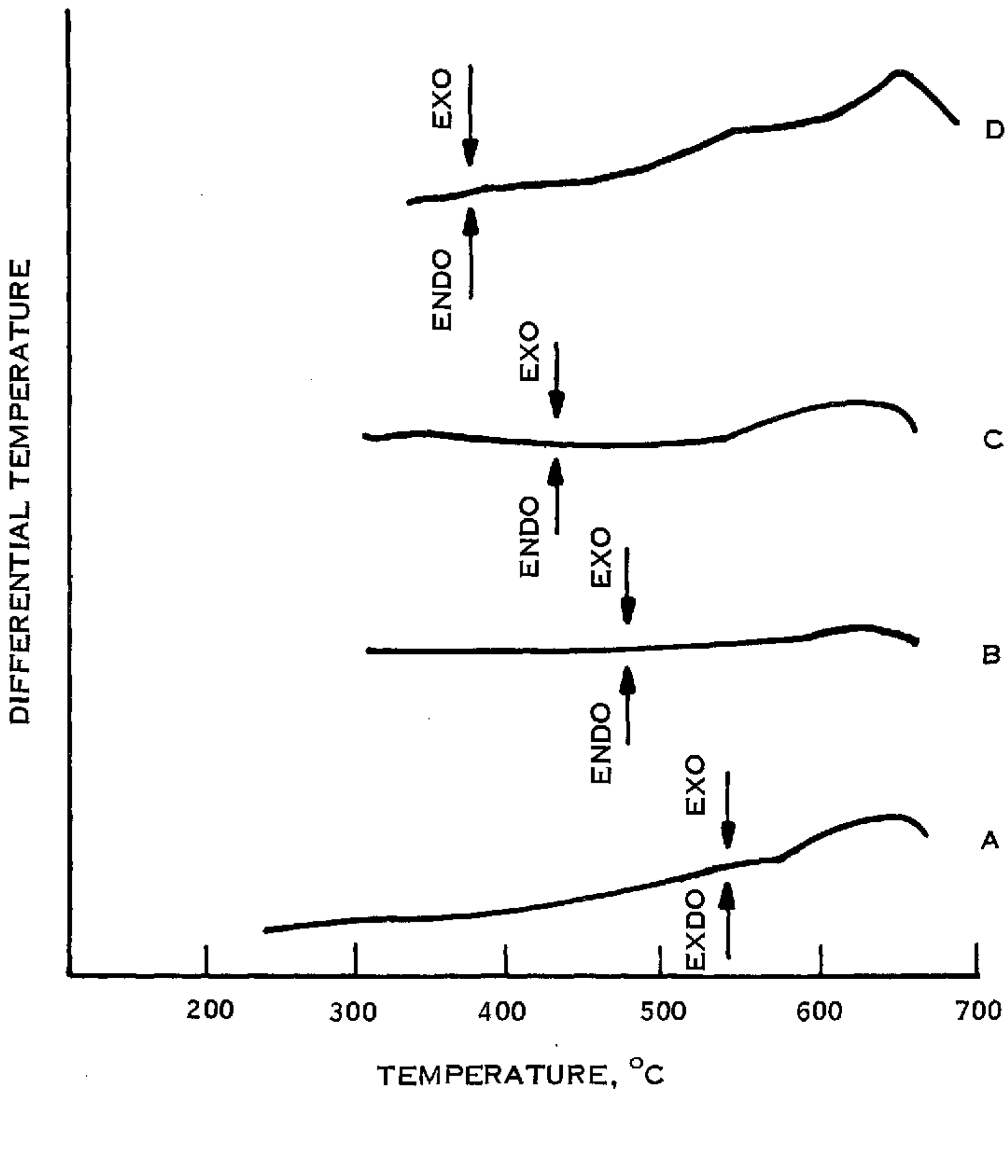

Figure 10. Details of the 74220,63 Glass for Different Thermal Histories: (A) As Received (45°C per second); (B) Cooled From 660°C at 0.1°C per Second; (C) Cooled From 660°C at 0.33°C per Second; (D) Cooled From 660°C at 48°C per Second.

For the orange soil, DTA revealed the existence of several exotherms - a small strain exotherm peaking at 640°C, another small exotherm at 755°C, as well as a much larger one occurring in the vicinity of 800°C. Samples to be studied by the Debye-Scherrer powder x-ray diffraction technique were heat treated in an argon atmosphere in the DTA cell at the appropriate temperatures for varying durations.

The measured "d" spacings are presented in Table 4. Except for samples heat treated at the highest temperature of 1120°C diffraction patterns were relatively weak and diffuse indicating a lack of crystallinity and were further obscured by fluorescence due to the presence of iron. In spite of these difficulties a possible interpretation of the thermal energy changes detected during DTA measurements has been arrived at by comparing the observed diffractional patterns with those listed in the ASTM powder diffraction file for various minerals reportedly[8, 9] present in orange soil. These patterns are presented in Table 5.

For the sample annealed 16 hours at 755°C, which is slightly higher in temperature than the first weak exotherm, there was the appearance of additional diffraction lines of "d" spacing, 3.18, 2.97, 2.64, 2.13, 2.02 and 1.68 Å. The best fit for these lines with the appropriate ratio of intensities was concluded to be the mineral diopside. The sample annealed for 2 hours at 855°C, a temperature slightly higher than that of the major exotherm, exhibited additional diffraction lines of "d" spacing 2.72, 3.70 and 1.86 Å. It is believed that the large exotherm represents the onset of crystallization of ilmenite, $FeTiO_3$, and this is further enhanced in the 1120°C annealed sample.

The samples annealed at low temperatures, 638°C and 710°C, produced especially diffuse diffraction patterns making identification extremely difficult. The presence of the mineral hypersthene could account for the observed lines, but a higher degree of crystallinity to provide sharper diffraction patterns is required for confirmation.

The minerals olivine and anorthite are reportedly[8, 9] present in orange soil on the basis of compositional and minerological evidence. However, their existence could not be established by x-ray diffraction study since all observed diffraction lines could be satisfactorally accounted for by the presence alone of ilmenite, diopside and hypersthene.

Table 4. X-ray Diffraction Data For Orange Soil Annealed at Various Temperatures (CuK_α rad., Ni Filter)

(3286) 638°C		(3320) 710°C, 23 hr.		(3309) 755°C 16 hr.		(3299) 855°C 2 hr.		(3287) 860°C		(3122) 1120°C	
d Å	I/I_o	d Å	I/I_o	d Å	I/I_o	d Å	I/I_o	d Å	I/I_o	d Å	I/I_o
						3.7	VVVW			3.62	VW
										3.41	VW
				3.18	VVW	3.2	VW	3.10	VVVW	3.18	MW
				2.97	VW	2.97	M	2.95	W	2.97	MS
		2.90	VVVW	2.89	VVVW	2.89	W	2.87	VVVW	2.86	M
2.77	VVVW			2.64	VVVW	2.72	VW	2.70	VVVW	2.70	M
2.50	VW	2.52	VVW	2.52	M	2.52	S			2.50	S
2.44	VW	2.43	VVW			2.48	W			2.44	VVW
				2.26	VVVW	2.24	VVW				
										2.19	W
				2.13	VVVW	2.12	VVVW	2.10	VVW	2.11	W
				2.02	VVVW	2.03	VVVW			2.01	W
						1.84	VVVW			1.84	MW
1.74	VVVW	1.74	VVVW	1.74	VVVW	1.74	VVW	1.74	VVVW	1.74	VW
				1.68	VVVW	1.67	VVW			1.68	VVW
1.64	VWW	1.62	VVVW	1.62	VW	1.62	W	1.63	VVW	1.62	M
										1.53	W
		1.48	VVVW	1.49	VVW	1.49	VW	1.49	VVW	1.50	W
				1.39	VVVW	1.42	VVVW	1.39	VVVW	1.41	VW
		1.31	VVVW	1.35	VVVW	1.33	VVVW				
				1.27	VVVW						

Table 5. ASTM Diffraction Patterns For Orange Soil Materials

3-0781 Ilmenite		19-239 Diopside		2-520 Hypersthene		20-20 Anorthite		9-369 Calcio-Olivine		Olivine 7-164 Fayalite		21-1260 Fosterite		21-1257 Halosiderite	
d Å	I/I_o	d Å	I/I_o	d Å	I/I_o	d Å	I/I_o	d Å	I/I_o	d Å	I/I_o	d Å	I/I_o	d Å	I/I_o
								5.63	40						
												5.10	20	5.16	13
						4.69	14								
								4.32	60						
						4.04	48	4.06	40						
						3.92	11					3.88	64	3.92	29
								3.82	60						
3.73	50					3.78	28	3.77	40	3.784	10	3.72	22	3.75	10
										3.558	30	3.50	15	3.52	36
						3.46	14					3.48	14		
		3.34	12	3.36	30	3.36	25	3.38	50						
						3.26	52								
		3.23	30	3.20	100	3.21	63	3.23	10						
						3.19	100								
						3.18	91								
						3.12	39								
		2.99	100	2.98	20	3.04	18	3.01	70	3.047	10	3.01	6	3.02	11
		2.95	30			2.95	27					2.991	18		
		2.894	40	2.898	80	2.934	19								
						2.828	20							2.791	78
2.74	100			2.73	30			2.75	60			2.764	62		
								2.73	100						
						2.655	14			2.634	20				
										2.621	20			2.603	11
2.54	85	2.566	25	2.55	50	2.526	20	2.54	20	2.566	50			2.533	71
		2.52	65			2.501	28	2.51	50	2.501	70	2.509	80		
								2.46	50			2.457	100	2.476	100
														2.371	13
												2.344	12		
										2.313	20	2.316	10		
		2.301	16							2.303	30				
												2.267	44	2.269	20
												2.246	30		
2.23	70			2.23	10										
		2.215	14												
		2.198	14												
												2.160	20	2.173	13
		2.133	18			2.142	17								
				2.11	50	2.095	10								
		2.04	20	2.03	20										
		2.014	14												
		2.006	10	1.96	40										
1.86	85					1.845	12								
		1.835	10			1.837	16								
1.72	100	1.754	14	1.78	40										
1.63	50	1.624	35	1.60	60										
				1.53	50										
1.50	85			1.498	80										
1.47	85														
				1.39	60										
1.34	70			1.34	30										
1.27	60			1.27	40										
				1.25	20										
1.20	30														
1.18	60			1.18	20										
1.15	70														
1.12	70														
1.07	70			1.05	40										

In Table 6, Debye-Scherrer powder x-ray diffraction data are presented for comparison of the SLG-17M synthetic glass with orange soil. Both materials after an 1120^{o}C, 2 hour heat treatment have not achieved a very high degree of crystallinity and the patterns are also partially obscured by a fluorescent background. Overall the data indicates a rather good correspondence. Most discrepancies occur in lines of weak intensity. However, it does appear that a slight difference in composition exists between the orange soil and the synthetic glass.

Several of the "as received" orange-red particles were identified under the metallurgical microscope and examined with the SEM. All particles examined in the sampling were spherical in shape.

A perfect spherical particle is shown in Figure 11A. At high magnification mounds become evident as in Figure 11B. Figure 11C shows a fragmented sphere. The fragmented area is shown in Figure 11D.

A red sphere with considerable surface structure is shown in Figure 11E. Details of the surface showing a splattered coating on the left and mounds on the right are shown in Figure 11D.

Three types of particles were observed after completion of the strain-relief exotherm and heat treatment to 685^{o}C. These were spheres (Figure 12), dumbbells (Figure 13) and non-spherical particles (Figure 14) of irregular shape.

A red spherical particle having what appears to be a conchoidal fracture is shown in Figure 12. Higher magnification (Figure 12B) shows micromounds producing a grainy texture. A pit is evident in the surface structure. High magnification of the sphere in Figure 12C shows mounds or spalls of several sizes on the glass surface as well as splash regions of glass (Figure 12D).

Table 6. Comparison of X-ray Diffraction Data for 1120°C, 2 Hr. Crystallized 74220,63 Orange Soil and SLG-17/ (CuK_α Rad., Ni Filter)

	SLG-17M		Orange Soil	
	d	I/I_o	d	I/I_o
			3.62	VW
	3.42	VW	3.41	VVW
	3.25	VVVW		
	3.16	VVVW	3.18	MW
(B)	2.94	W	2.97	MS
	2.85	VVW	2.86	M
	2.72	VVW	2.70	M
(VB)	2.51	M	2.50	S
			2.44	WW
			2.27	VVW
	2.18	VVVW	2.19	W
	2.12	VVVW	2.11	W
			2.01	W
	1.96	VVVW		
	1.84	VVW	1.84	MW
	1.73	VVVW	1.74	VW
	1.66	VVVW	1.68	VVW
(VB)	1.62	W	1.62	W
(B)	1.53	VW	1.53	VW
			1.50	W
	1.475	VVW		
	1.41	VVVW	1.41	VW
	1.38	VVVW		

Figure 11. "As-Received" 74220,63 Orange-Red Spheres.

(A) Unfragmented Particle at 3200X
(B) Surface Mounds on Sphere in (A) at 10,000X
(C) Fragmented Sphere at 1000X
(D) Surface of Fragmented Area at 3000X
(E) Sphere Containing Considerable Surface Structure at 2000X, and
(F) 5000X

These Particles are Representative of the "As Received" Orange Soil and Were Not Subjected to Heat Treatment.

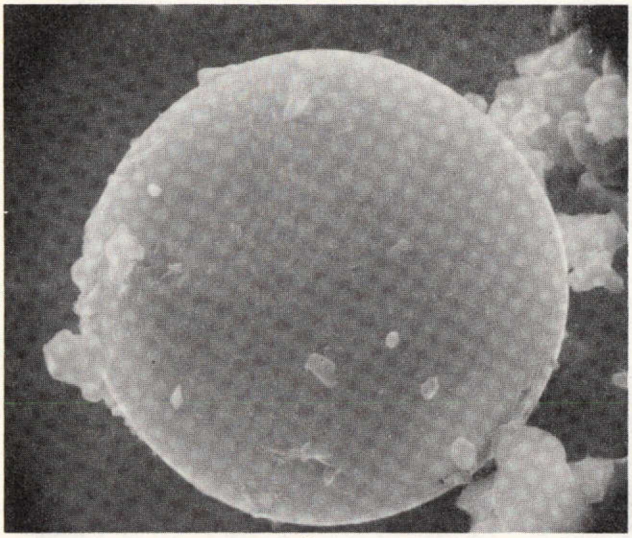

A

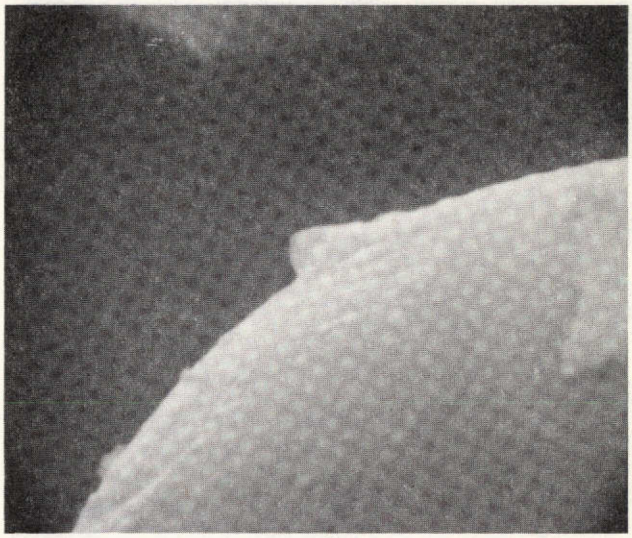

B

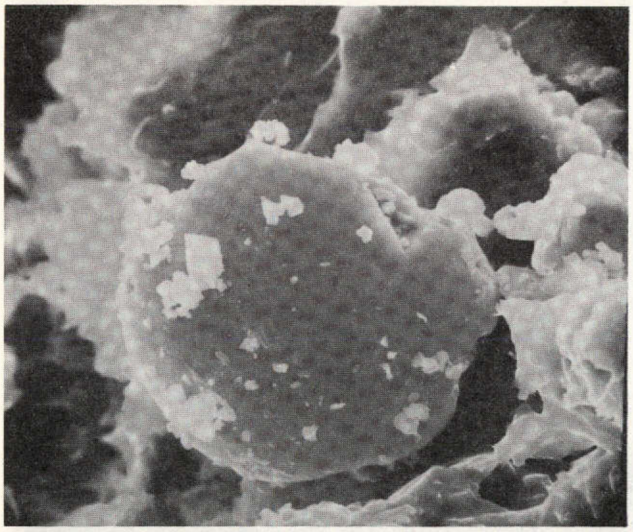

C

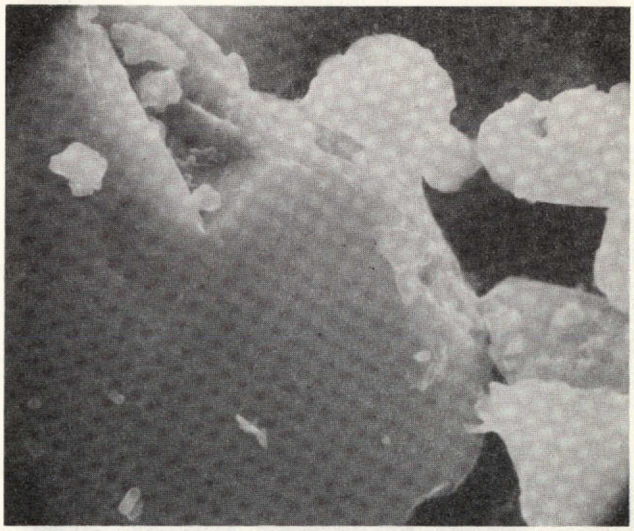

D

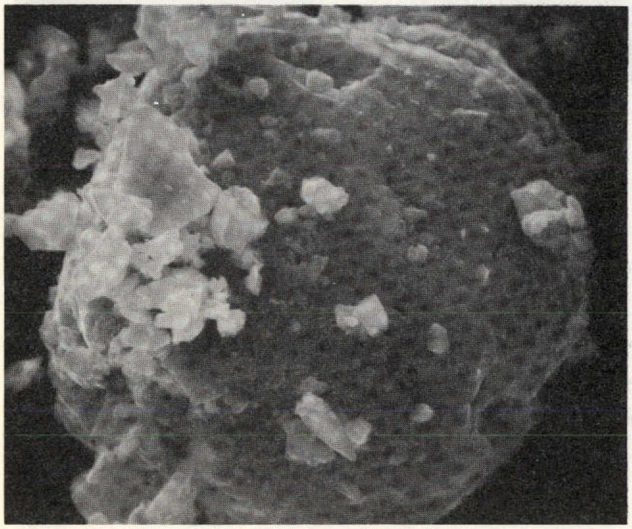

E

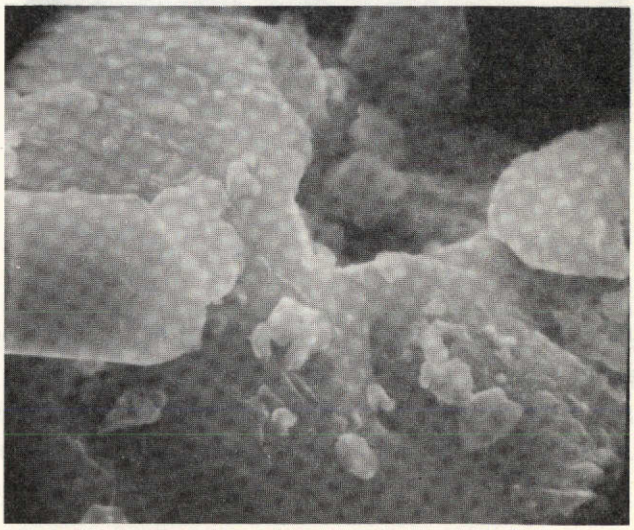

F

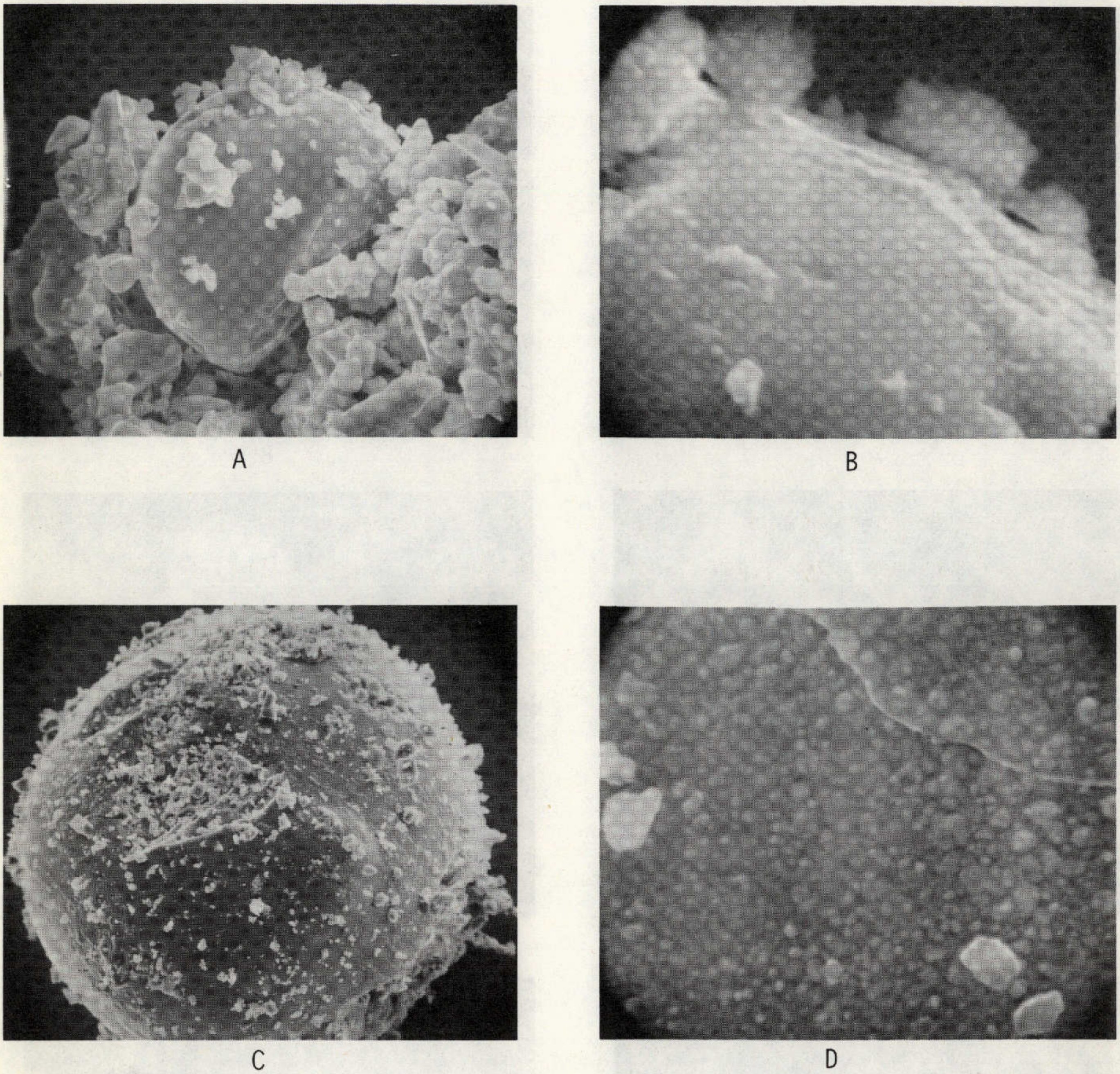

Figure 12. Particles of the 74220, 63 Orange Soil Which Were Heat Treated in the DTA to 685^{o}C to Examine Surface Structural Development Associated With the Strain Relief Exotherm (See Figure 8). (A) Sphere Showing Conchoidal Fracture at 2000X. (B) Grainy Texture at 10, 000X; (C) Splash Regions and Spalls on Spheres at 470X and (D) 10, 000X.

The features on the spheres suggest that hot glass spheres may have been impacted by molten glass, solid glass, or solid-liquid combinations at low velocities. It is likely that during the impact sequence some spheres could cool to a glass and be fractured or spalled by the continuing impacts after solidification. This is suggested by the sphere in Figure 12A.

Dumbbells have also been a common form of lunar galss geometry. Figure 13A shows a black particle which consists of two joined dumbbell particles. Figures 13B and 13C show the surfaces at higher magnification after rotation and at a 76° tilt. Of interest is the coating which covers both dumbbell surfaces. Another view of the joined particles in proximity of the coating is shown in Figure 13D. High magnification shows that the two dumbbells show a complete fusion and joining. Both surfaces are free from surface effects except for the micromounds on the surface. A crevice is shown across the field of view (Figure 13E).

The irregularly-shaped particles (Figure 14A and 14C), red-orange under the metallurgical light microscope, are shown at high magnification in Figures 14B and 14D. The particle in Figure 14B has well-defined sharp edges, suggesting fragmentation in the quenched condition. These well-defined features are absent in the particle in Figures 14C and 14D. A flow-pattern appears left of center in Figure 14C. This suggests that the particle experienced flow relaxation and deformation during high temperature exposure; these processes may have occurred during the DTA run and be associated with the accentuated exotherm of strain relief.

Figure 15 shows an overview of the mounted particles from the sample fired to 860°C in the DTA. As shown in Figure 8, this temperature represents completion of the two exothermic peaks of crystallization. There are still a few perfect spheres and an unbroken double dumbbell (lower right) which seem to be unaffected by heat treatment to 860°C. However, many deformed particles of irregular shape can now be observed. These are shown at high magnification in Figures 16 and 17 and, based on the surface morphologies, are considered to be at least partially recrystallized. This is verified by the x-ray data presented in the next section.

Figure 13. Dumbbells Have Been a Common Form of Lunar Glass Geometry. This Figures Shows a Black Particle of 74220,63 at (A) 470X and (B) 570X Which Was Heat Treated in the DTA to 685°C and Consists of Two Joined Dumbbells. The Join and a Surface Coating After Rotation and at a 76° Tilt is Shown in (C) at 1150X. Another View of the Joined Dumbbells in Proximity of the Coating at 1150X (D) Shows Complete Fusion and Joining. (E) Shows a Crevice Across the Field of View at 11,800X.

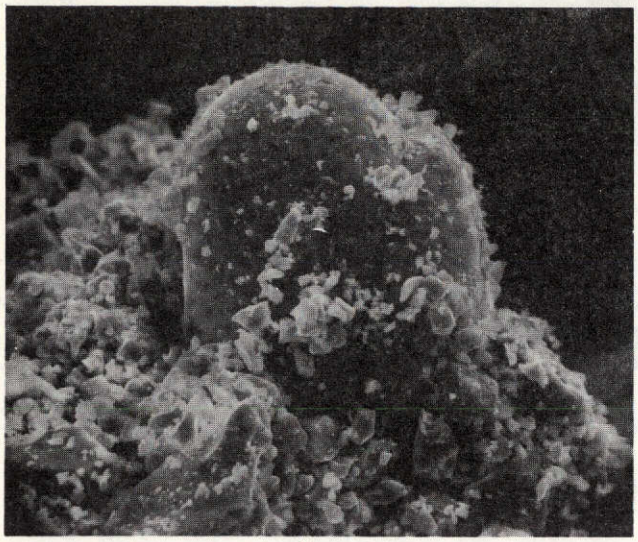

A

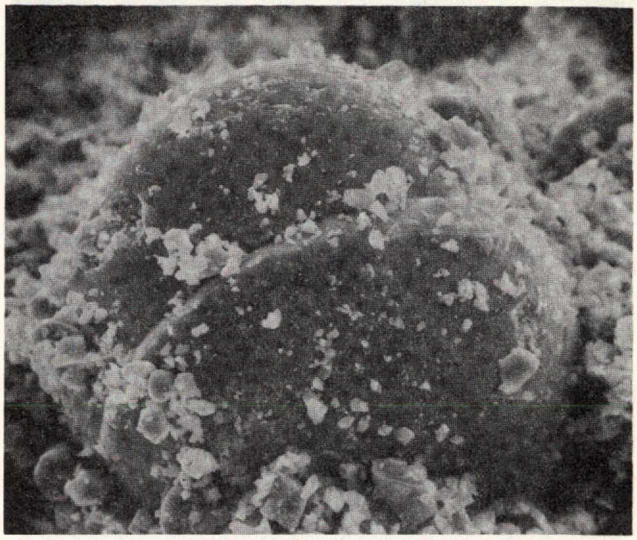

B

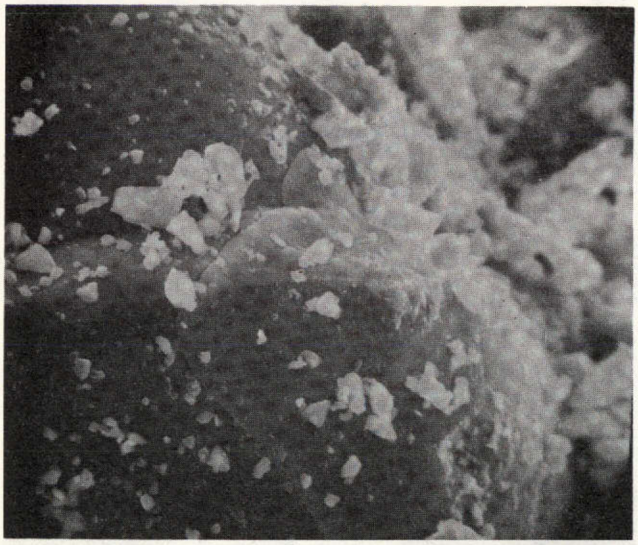

C

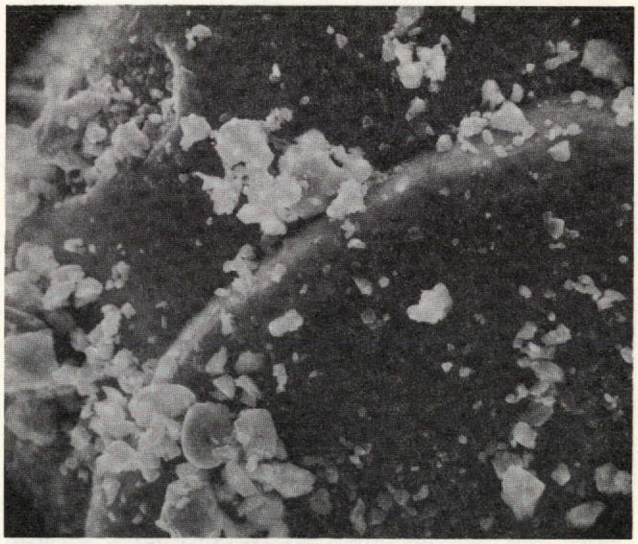

D

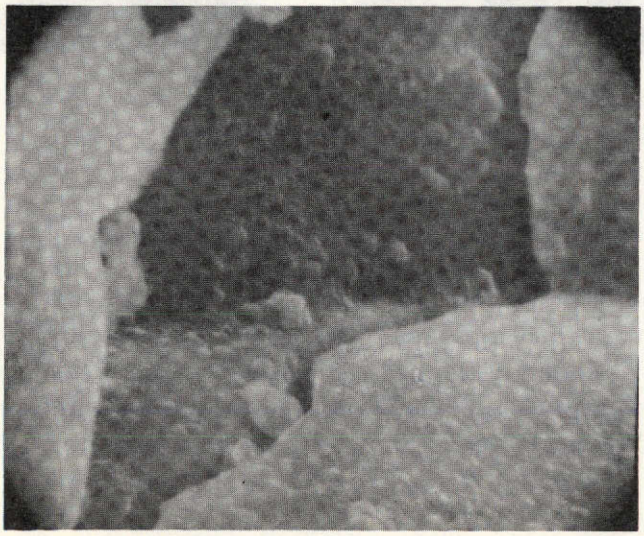

E

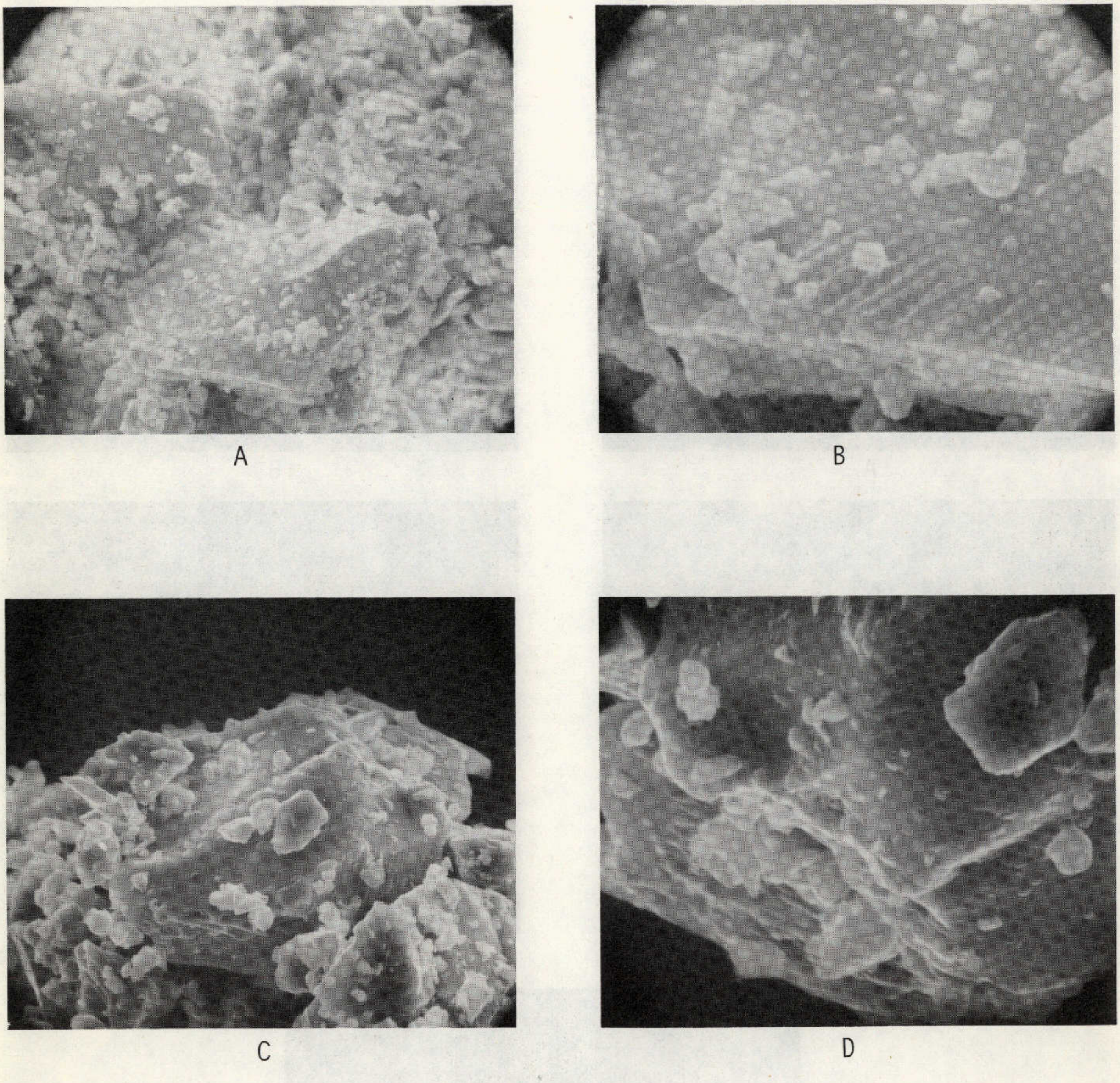

Figure 14. Non-spherical Particles of 74220, 63 Which Have Been Subjected to 685°C in the DTA. Flow and Deformation Processes are Suggested Which May be Associated With the Accentuated Exotherm of Strain-Relief. (A) Red-Orange Particle at 2000X Has Well-Defined, Sharp Features as Shown in (B) at 5000X. (C) Red-Orange Particle at 2000X Which Has Experienced Flow and Relaxation As Shown in (D) at 5000X.

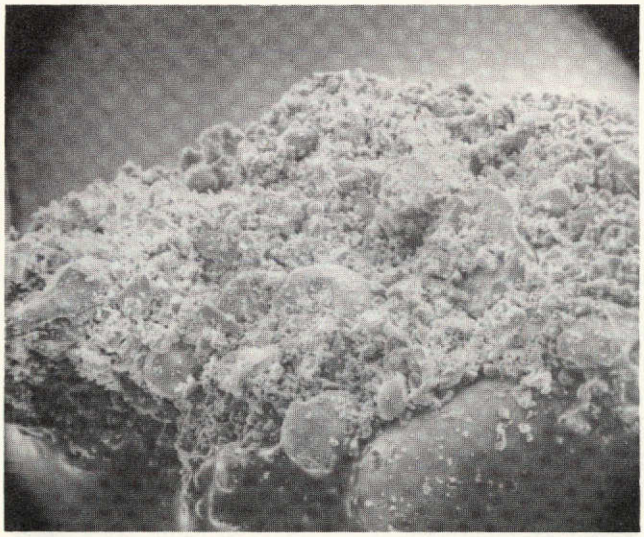

Figure 15. Overview of Mounted 74220, 63 Particles Which Have Experienced the DTA Crystallization Exotherms to 860°C. Note the Unfractured Dumbbell at Lower Right. 200X

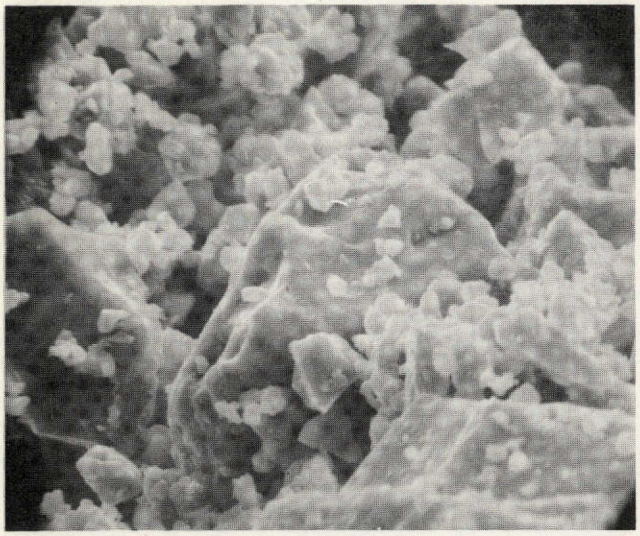

A

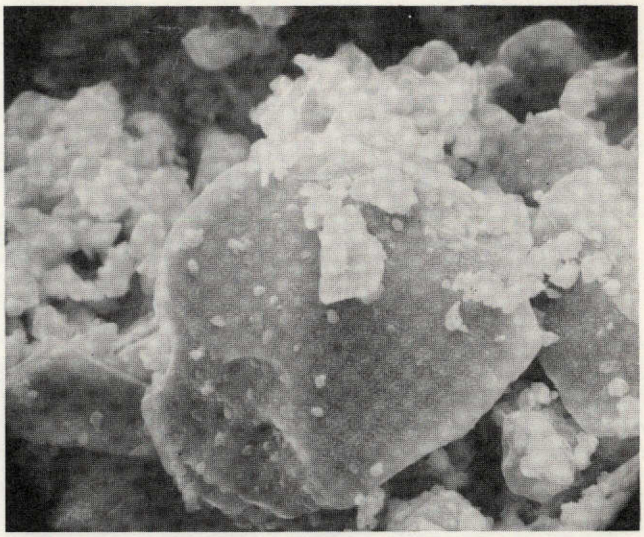

B

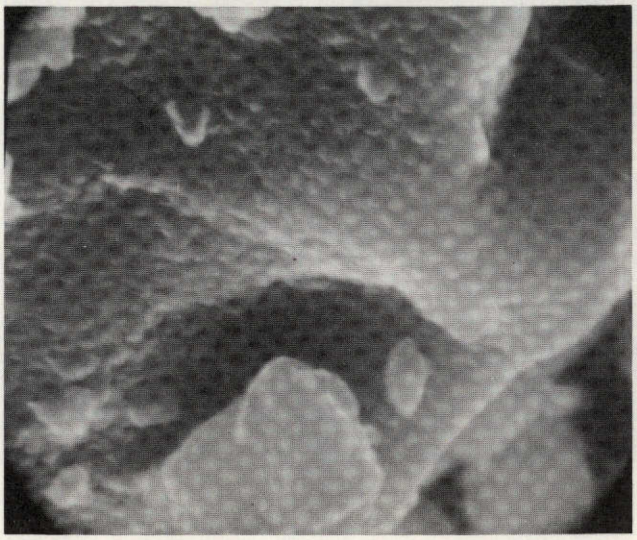

C

Figure 16. Deformed Orange-Red Particles of 74220,63 Which Have Been Subjected to DTA to 860°C. They Have Experienced the Exotherms of Crystallization. A Fine-Grained Texture of Micromounds on What May be Partially Collapsed Spheres are Shown in (A) 2000X and (B) 1600X for Two Spheres: (C) is the Surface of Sphere (A) at 10,000X

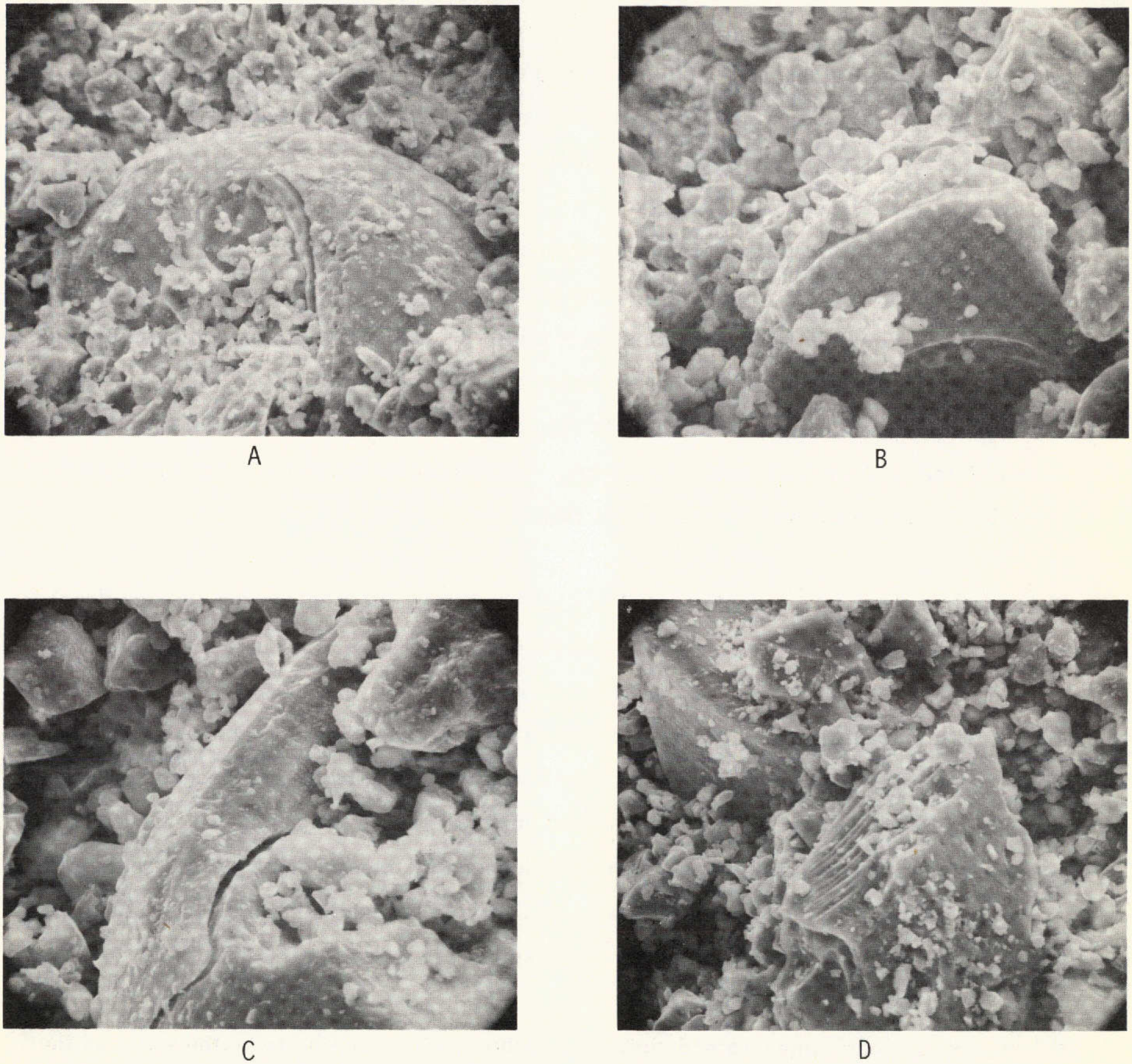

Figure 17. Fractured and Broken 74220,63 Particles. These Particles Have Experienced the DTA Crystallization Exotherms to 860^{o}C. (A) Sphere Supporting Shell of Second Sphere (1000X); (B) Partially Deformed Orange Dumbbell (2000X); (C) Fractured Dumbbell Showing Micromounds and Splattering (1600X); (D) Fragment Showing Texture Similar to that of 64455,21 After Completion of DTA Exotherm (800X).

For example, the orange-red particles in Figure 16 show a fine-grained texture of micromounds on what may be partially collapsed spheres. According to Cadenhead[10], hollow spheres are consistent with volcanic origin.

Figure 17A shows a partially deformed, broken sphere which appears to be supporting the shell of a second sphere. Figures 17B and 17C show a partially deformed, broken orange-red dumbbell. Each of these particles show similar surface morphologies consisting of partially devitrified splattered glass and micromounds. The particle in Figure 17D shows a texture on the original surface which is similar to that observed on 64455, 21 after completion of the DTA crystallization exotherm. This is discussed in the previous section. Substructure is absent on the fracture surface in Figure 17D.

Examination of the DTA sample heated to 1120°C showed that sintering of the individual particles had taken place between 860° and 1200°C. The sinter products were black and had a dark vesicular appearance. Carter has reported that vesicular particles are consistent with volcanic origin[11]. The particle in Figures 18A and 18B show spherical impressions in the surface and a sphere in the lower left which is still embedded. There appears to be a fine-grained structure on the surface. Dendritic needle-like crystals appear to have formed within the particles as evidenced by the structure within the depressions and the open voids. Another view of this sample at high magnification (Figure 18C) shows that indeed rectangular bar-shaped crystals to exist within the void.

Other particles have fine-grained surface structures which appear to be the same as the first particle; however, the spherical depressions are fewer in number and smaller in size. EDX of the area showed Fe, Ti, Ca, Si, Mg and Al in major proportions and Cr and Mn in minor amounts.

The particle in Figure 18D contained depressions similar to the first and offered an excellent opportunity to observe the bar-shaped crystals within the depression. This is shown in Figure 18E.

The particle in Figure 19A did not contain spherical depressions. However, examination of the void area shown in Figure 19B revealed two observations. First, the bar-like crystals appear to have started to melt at these temperatures (Figure 19C). This is indicated by the rounded corners of the bars. Second, a well-defined crystal, approximating a rhombahedron, was observed as shown in Figure 19D. Energy dispersive analysis showed Fe, Ti, Ca, Si, Mg and Al to be all present as major elements with Cr and Mn present in minor amounts. However, energy dispersive analysis shows that the crystals shown in Figure 18C have Fe, Ti, Ca and Si in major amounts with Al and Mg present in lesser quantities. Also detected were Cr and Mn.

Figure 18. Particles of 74220,63 Which had Been Heat Treated to 1120°C in the DTA Were Sintered With a Dark Vesicular Appearance. The Particle in (A) at 500X Shows Spherical Impressions in the Surface and (B) an Embedded Sphere at 1000X. (C) Rectangular Bar Shaped Crystals Within Void on Surface (5000X). (D) A Second Particle at 500X Showing Crystals. (E) in Void at 5000X.

A

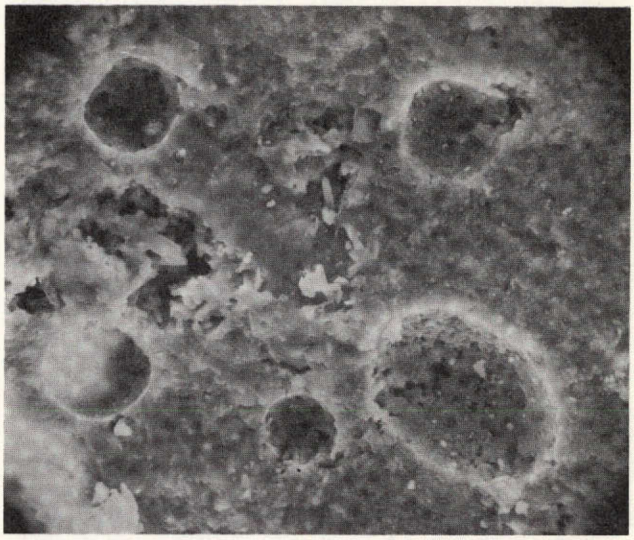

B

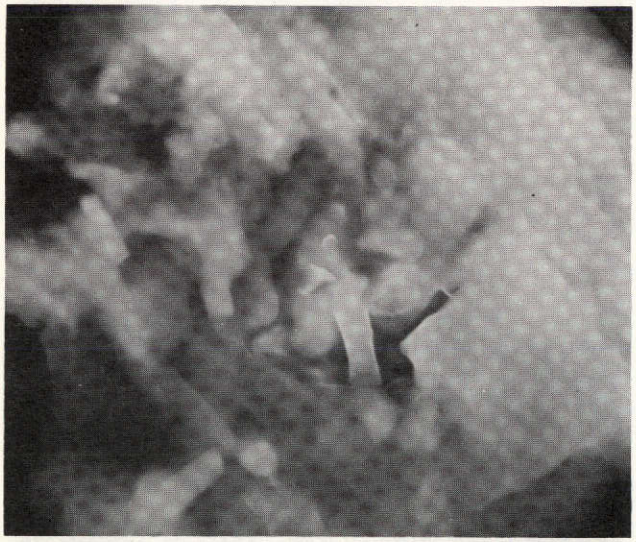

C

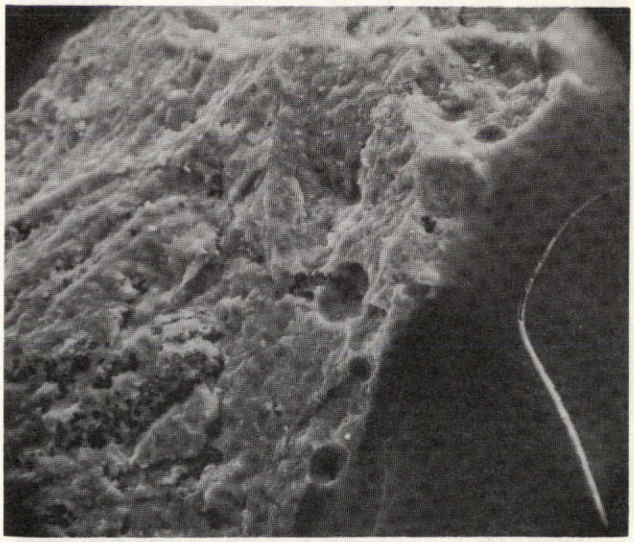

D

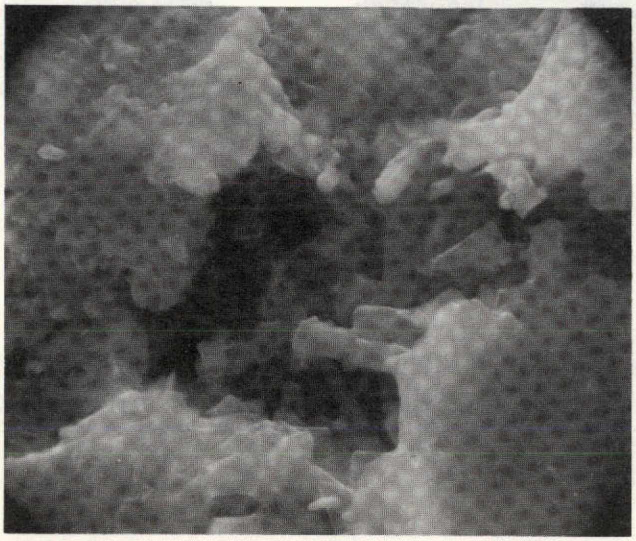

E

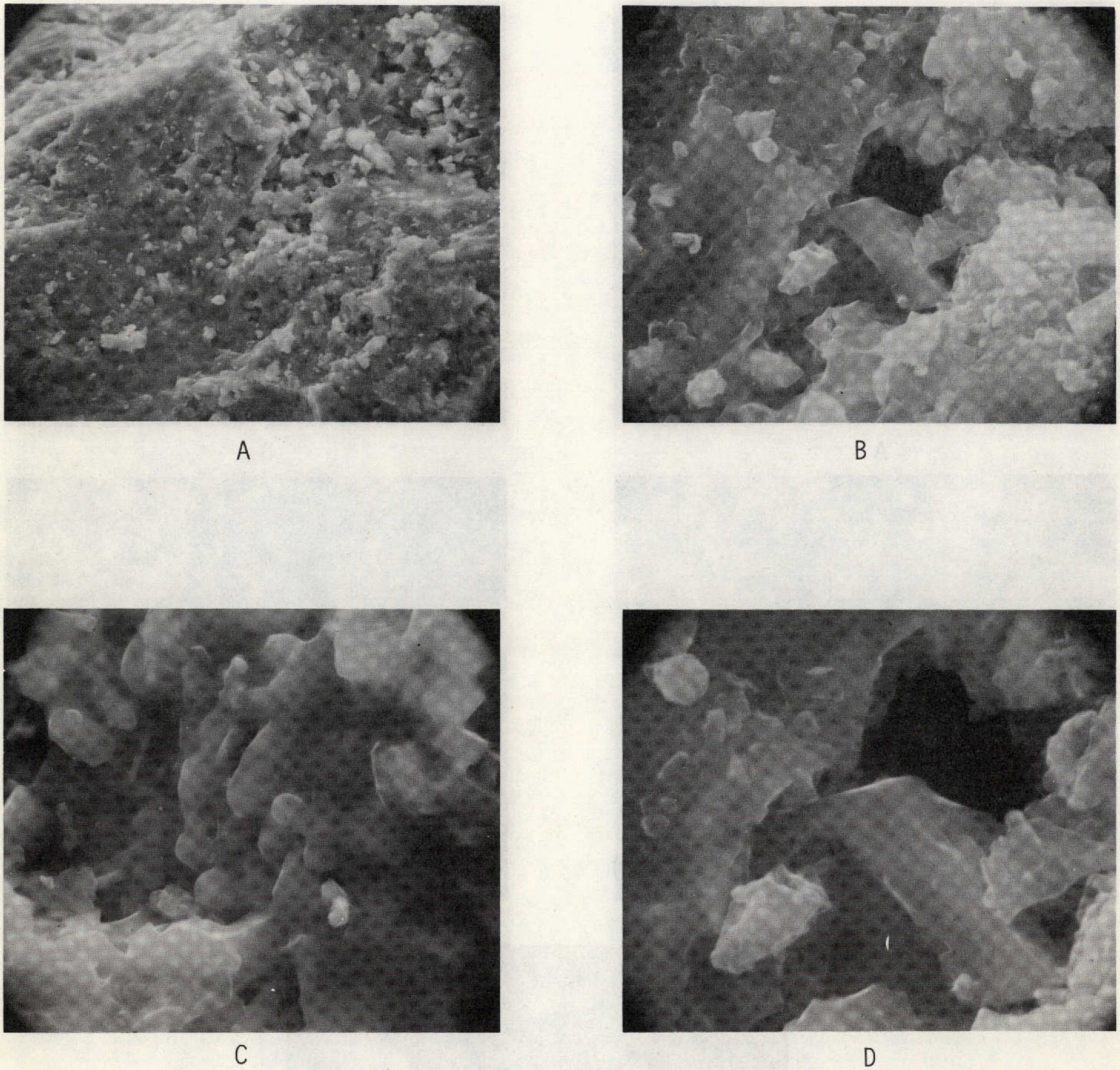

Figure 19. Particles of 74220, 63 Which had Been Heat Treated to 1120°C in the DTA Were Sintered Without Spherical Surface Depressions. (A) Surface at 1000X; (B) Void Area at 5000X Showing; (C) Bar-Like Crystals at 5000X Which Have Started to Melt and (D) a Well, Defined Rhombohedron Crystal at 10, 000X

SECTION 4

SUMMARY AND INTERPRETATION OF RESULTS

Synthetic glasses have been processed which are of essentially the same composition as the Apollo 16 64455, 21 and Apollo 17 74220, 63 lunar glasses. The similarity in differential thermal analyses profiles between the lunar glasses and their synthetic analogs is striking. The lunar glasses showed accentuated exotherms of strain relief in the annealing range, indicating that the last cooling rate of each had been rapid. It is fortunate that the lunar samples studied show evidence for strain in their structure which is amenable to interpretation by comparison to the known history of the synthetic glasses. On this basis the rates of quench from the melt which show the closest match between the lunar and synthetic glasses are, respectively, 8^{o} and $45^{o}C$ per second for the 64455, 21 and 74220, 63 glasses. It is expected that the cooling rates between these two specimens differed by an order of magnitude because of the difference in the masses involved.

The study of the relationship of the strain-relief exotherm to the quench rate from which the strain originated shows that for both the 64455, 21 and 74220, 63 glasses there is a minimum cooling rate below which no strain is introduced. This falls between 0.1^{o} to $0.33^{o}C$ per second. The upper limits have not been determined because there appears to be a maximum amount of strain that can be built into these particular structures such that higher quench rates do not produce detectable changes in the glass.

There is a significant difference in the temperatures of crystallization of the 64455, 21 and 74220, 63 glasses. The 64455, 21 shows an exotherm which peaks at $935^{o}C$ and is complete by $970^{o}C$. This can be correlated with heating on the SEM hot stage; a change in surface morphology is observed between 960^{o} and $975^{o}C$. A convoluted, ropy structure develops with the surface having partially deformed and crystallized. By $1200^{o}C$ a recrystallized glass surface containing "splash-like" features rich in Si, Ca, and Al and deficient in Fe has developed. Spherical particles are embedded in the "splash" area which are rich in Ni and Fe.

The best x-ray diffraction pattern fit for the Apollo 16 crystallization is one of several plagioclase feldspars. Since the lunar glass is outstandingly richer in CaO than the Na_2O, this narrows the choice of plagioclase mineral to either bytownite or anorthite. The close correspondence that exists between the diffraction data for bytownite and the Apollo 16 lunar glass was particularly evident.

The 74220, 63 showed a minor exotherm of crystallization peaking at 750°C and a major exotherm of crystallization peaking at 800°C. The former corresponded to the crystallization of diopside and the latter to ilmenite. Ilmenite was further developed with heat treatment to 1120°C. Samples annealed at 638° and 710°C showed diffuse patterns. Hypersthene could possibly account for the observed lines. All observed diffraction lines could be satisfactorily accounted for by the presence of diopside, hypersthene and ilmenite. The presence of olivine or anorthite could not be established.

The strain-relief mechanism appears to have no observable effect on the surface morphologies of the spheres, fragmented spheres, dumbbells and non-spherical particles. Speculation has been made as to origin from several interesting substructures which have been observed, but these relate most likely to the "as cooled" condition.

After completion of the two exothermic peaks of crystallization, many deformed particles of irregular shape can be observed. These appear to be partially recrystallized, and, in some cases, partially collapsed spheres. Sintering of the individual particles takes place between 860° and 1200°C. The products have a dark vesicular appearance, spherical surface depressions, a fine-grained surface texture, and needle-like or bar-like crystals which can be observed through the depressions.

The data reported to date, particularly on Apollo 11 and Apollo 12 samples, indicate that lunar glass spherules were cooled rapidly through the glass-transition temperature range (500° to 800°C) during their most recent cooling[12,13,14]. Cooper, et al have reported, based on index of refraction and density changes with heat treatment in Apollo 11 and Apollo 12 glasses, that the increases are extraordinarily large when compared to the usual glass-transition phenomena[14]. They calculated that a 2% change in density is equivalent to an increase of 330°C in the glass-transition temperature, Tg. Cooling rates of $> 10^5$°C per second would be required to extend the glass transition temperature by such an amount. Estimates of radiation cooling of a lunar sphere of emissivity 0.5 and diameter 50 microns gave a cooling rate of $< 10^3$ per second.[15] Thus, a good quantitative agreement between the present results and the accepted kinetic theory of the glass transition cannot be claimed[16].

Roedder and Weiblen[17] have estimated that cooling rates in excess of $1000^{o}C$ per second were needed to maintain the Apollo 17 orange glass spherules as glass. They cited that a melt of this composition can be expected to nucleate and crystallize much more rapidly than ordinary terrestrial glasses.

We cannot say that the 74220, 63 particles were formed at $1000^{o}C$ per second as reported by Roedder[17], but, based on our own glass formulating experience and the rates established for glass formation in this study, these rates ($1000^{o}C$ per second) appear to be too high.

Surface microstructures were formed on both glasses after the crystallization exothermic reactions. However, no morphologies appear to have formed as a result of strain relief. These features formed in the 74220, 63 particles after crystallization and sintering are similar to features associated with volcanic mechanisms[11]. The rates of cooling of the 64455, 21 glass and the formation of the Ni-Fe spheres with crystallization treatment are suggestive of impact mechanisms of formation or impact related events.

SECTION 5

REFERENCES

1. Phenney, W.C., compiler, "Summary of Apollo 17 Preliminary Examination Team Results," March 5, 1973.

2. Tool, A.Q. and Eichlin, C.G., J. Opt. Soc. Amer., Vol. 4, No. 340, 1920.

3. Stanworth, J.E., Physical Properties of Glass, Oxford, pp. 158-169, 1953.

4. McKay, D.S. and Laydle, G.H., "Scanning Electron Microscopy Study of Particles in Lunar Soil," Proc. Fourth Annual SEM Symposium, IITRI, Chicago, pp. 172-184, 1971.

5. Grieve, R.A.F. and Plant, A.G., Paper 64455, presented at Fourth Lunar Science Conference, March 1973.

6. Samsonov, G.V., The Oxide Handbook, IFI Plenum, pp. 264-272, 1973.

7. McKay, K.G., "Secondary Electron Emission," Advances in Electronics, Vol. 1, Academic Press, pp. 75-76, 1948.

8. Science, Vol. 182, pp. 659-690, Nov. 16, 1973.

9. Reid, A.M., Lofgren, G.E., Heiken, G.H., Brown, R.W. and Moreland, G., Trans. Amer. Geophysical Union, Vol. 54, No. 6, pp. 607, June 1973.

10. Cadenhead, D.A., Trans. American Geophysical Union, Vol. 54, No. 6, pp. 582, 1973.

11. Carter, J.L., Taylor, H.C. and Padovani, E., Trans. American Geophysical Union, Vol. 54, No. 6, pp. 582, 1973.

12. Greene, C.H., Pye, L.D., Stevens, H.J., Rase, D.E. and Kay, H.S., Proc. Second Lunar Sci. Conf., No. 3, pp. 2049-55 (1971).

13. Roy, R., Roy, D.M., Kurtossy, S. and Faite, S.P., ibid, pp. 2069-78.

14. Cooper, A.R., Varshneya, A.K., Sarkar, S.K., Swift, J., Klein, L. and Yen, F., J. Amer. Ceram. Soc., Vol. 55, No. 5, 260-264 (1972).

15. Isard, J., Proc. Second Lunar Sci. Conf., Vol. 3, pp. 2003-2008, 1971.

16. Litovitz, T.A., pp. 252-68 in Non-Crystalline Solids, edited by V.D. Frechette, John Wiley & Sons, Inc., New York, 1960.

17. Roedder, E. and Weiblen, P.U., Nature, No. 244, pp. 210-212, July 27, 1973.